

Robustness of Conditional GANs to Noisy Labels

Kiran Koshy Thekumparampil[†], Ashish Khetan[†], Zinan Lin[‡], Sewoong Oh[†]

[†]University of Illinois at Urbana-Champaign, [‡]Carnegie Mellon University

Abstract

We study the problem of learning conditional generators from noisy labeled samples, where the labels are corrupted by random noise. A standard training of conditional GANs will not only produce samples with wrong labels, but also generate poor quality samples. We consider two scenarios, depending on whether the noise model is known or not. When the distribution of the noise is known, we introduce a novel architecture which we call Robust Conditional GAN (RCGAN). The main idea is to corrupt the label of the generated sample before feeding to the adversarial discriminator, forcing the generator to produce samples with clean labels. This approach of passing through a matching noisy channel is justified by corresponding multiplicative approximation bounds between the loss of the RCGAN and the distance between the clean real distribution and the generator distribution. This shows that the proposed approach is robust, when used with a carefully chosen discriminator architecture, known as projection discriminator. When the distribution of the noise is not known, we provide an extension of our architecture, which we call RCGAN-U, that learns the noise model simultaneously while training the generator. We show experimentally on MNIST and CIFAR-10 datasets that both the approaches consistently improve upon baseline approaches, and RCGAN-U closely matches the performance of RCGAN.

1 Introduction

Conditional generative adversarial networks (GAN) have been widely successful in several applications including improving image quality, semi-supervised learning, reinforcement learning, category transformation, style transfer, image de-noising, compression, in-painting, and super-resolution [30, 13, 48, 36, 26, 58]. The goal of training a conditional GAN is to generate samples from distributions satisfying certain *conditioning* on some correlated features. Concretely, given samples from joint distribution of a data point x and a label y , we want to learn to generate samples from the true conditional distribution of the real data $P_{X|Y}$. A canonical conditional GAN studied in literature is the case of discrete label y [30, 36, 35, 32]. Significant progresses have been made in this setting, which are typically evaluated on the quality of the conditional samples. These include measuring inception scores and intra Fréchet inception distances, visual inspection on downstream tasks such as category morphing and super resolution [32], and faithfulness of the samples as measured by how accurately we can infer the class that generated the sample [36].

We study the problem of training conditional GANs with noisy discrete labels. By noisy labels, we refer to a setting where the label y for each example in the training set is randomly corrupted. Such noise can result from an adversary deliberately corrupting the data [7] or from human errors in crowdsourced label collection [12, 18]. This can be modeled as a random process, where a clean data point $x \in \mathcal{X}$ and its label $y \in [m]$ are drawn from a joint distribution $P_{X,Y}$ with m classes. For each data point, the label is corrupted by passing through a noisy channel represented by a row-stochastic *confusion matrix* $C \in \mathbb{R}^{m \times m}$ defined as

Author emails are thekump2@illinois.edu, khetan2@illinois.edu, zinanol@andrew.cmu.edu, and swoh@illinois.edu. This work used the Extreme Science and Engineering Discovery Environment (XSEDE), which is supported by National Science Foundation grant number OCI-1053575. Specifically, it used the Bridges system, which is supported by NSF award number ACI-1445606, at the Pittsburgh Supercomputing Center (PSC).

$C_{ij} \triangleq \mathbb{P}(\tilde{Y} = j | Y = i)$. This defines a joint distribution for the data point x and a noisy label \tilde{y} : $\tilde{P}_{X,\tilde{Y}}$. If we train a standard conditional GAN on noisy samples, then it solves the following optimization:

$$\min_{G \in \mathcal{G}} \max_{D \in \mathcal{F}} V(G, D) = \mathbb{E}_{(x, \tilde{y}) \sim \tilde{P}_{X,\tilde{Y}}} [\phi(D(x, \tilde{y}))] + \mathbb{E}_{z \sim N, y \sim \tilde{P}_{\tilde{Y}}} [\phi(1 - D(G(z; y), y))] \quad (1)$$

where ϕ is a function of choice, D and G are the discriminator and the generator respectively optimized over function classes \mathcal{G} and \mathcal{F} of our choice, and N is the distribution of the latent random vector. For typical choices of ϕ , for example $\log(\cdot)$, and large enough function classes \mathcal{G} and \mathcal{F} , the optimal conditional generator learns to generate samples from $\tilde{P}_{X|\tilde{Y}}$, the corrupted conditional distribution. In other words, it generates samples X from classes other than what it is conditioned on. As the learned distribution exhibits such a bias, we call this naive approach the *Biased GAN*. Under this setting, there is a fundamental question of interest: can we design a novel conditional GAN that can generate samples from the true conditional distribution $P_{X|Y}$, even when trained on noisy samples?

Several aspects of this problem make it challenging and interesting. First, the performance of such robust GAN should depend on how noisy the channel C is. If C is rank-deficient, for instance, then there are multiple distributions that result in the same distribution after the corruption, and hence no reliable learning of the true distribution is possible. We would ideally want a theoretical guarantee that shows such trade-off between C and the robustness of GANs. Next, when the noise is from errors in crowdsourced labels, we might have some access to the confusion matrix C from historical data. On other cases of adversarial corruption, we might not have any information of C . We want to provide robust solutions to both. Finally, an important practical challenge in this setting is to correct the noisy labels in the training data. We address all such variations in our approaches and make the following contributions.

Our contributions. We introduce two architectures to train conditional GANs with noisy samples.

First, when we have the knowledge of the confusion matrix C , we propose RCGAN (Robust Conditional GAN) in Section 2. We first prove that minimizing the RCGAN loss provably recovers the clean distribution $P_{X|Y}$ (Theorem 2), under certain conditions on the class \mathcal{F} of discriminators we optimize over (Assumption 1). We show that such a condition on \mathcal{F} is also necessary, as without it, the training loss can be arbitrarily small while the generated distribution can be far from the real (Theorem 3). The assumption leads to our particular choice of the discriminator in RCGAN, called *projection discriminator* [32] that satisfies all the conditions (Remark 2). Finally, we provide a finite sample generalization bound showing that the loss minimized in training RCGAN does generalize, and results in the learned distribution being close to the clean conditional distribution $P_{X|Y}$ (Theorem 4). Experimental results in benchmark datasets confirm that RCGAN is robust against noisy samples, and improves significantly over the naive Biased GAN.

Secondly, when we do not have access to C , we propose RCGAN-U (RCGAN with Unknown noise distribution) in Section 4. We provide experimental results showing that performance gains similar to that of RCGAN can be achieved. Finally, we showcase the practical use of thus learned conditional GANs, by using it to fix the noisy labels in the training data. Numerical experiments confirm that the RCGAN framework provides a more robust approach to correcting the noisy labels, compared to the state-of-the-art methods that rely only on discriminators.

Related work. Two popular training methods for generative models are variational auto-encoders [22] and adversarial training [14]. The adversarial training approach has made significant advances in several applications of practical interest. [37, 2, 5] propose new architectures that significantly improve the training in practical image datasets. [58, 16] propose new architectures to transfer the style of one image to the other domain. [26, 43] show how to enhance a given image with learned generator, by enhancing the resolution or making it more realistic. [27, 50] show how to generate videos and [51, 1] demonstrate that 3-dimensional models can be generated from adversarial training. [23] proposes a new architecture encoding causal structures in conditional GANs. [42] introduces the state-of-the-art conditional independence tester. On a different direction, several recent approaches showcase how the manifold learned by the adversarial training can be used to solve inverse problems [9, 57, 53, 49].

Conditional GANs have been proposed as a successful tool for various applications, including class conditional image generation [36], image to image translation [21], and image generation from text [38, 55]. Most of the conditional GANs incorporate the class information by naively concatenating it to the input or feature vector at some middle layer [30, 13, 38, 55]. AC-GANs [36] creates an auxiliary classifier to incorporate class information. Projection discriminator GAN [32] takes an inner product between the embedded class vector and the feature vector. A recent work [31] which proposes spectral normalization shows that high quality image generation on 1000-class ILSVRC2012 dataset [39] can be achieved using projection conditional discriminator.

Robustness of (unconditional) GANs against adversarial or random noise has recently been studied in [10, 52]. [52] studies an adversary attacking the output of the discriminator, perturbing the discriminator output with random noise. The proposed architecture of RCGAN is inspired by a closely related work of AmbientGAN in [10]. AmbientGAN is a general framework addressing any corruption on the data itself (not necessarily just the labels). Given a corrupted samples with known corruption, AmbientGAN applies that corruption to the output of the generator before feeding them to the discriminator. This has shown to successfully de-noise images in several practical scenarios.

Motivated by the success of AmbientGAN in de-noising, we propose RCGAN. An important distinction is that we make specific architectural choices guided by our theoretical analysis that gives a significant gain in practice as shown in Section 6. Under the scenario of interest with noisy labels, we provide sharp analyses for both the population loss and the finite sample loss. Such sharp characterizations do not exist for the more general AmbientGAN scenarios. Further, our RCGAN-U does not require the knowledge of the confusion matrix, departing from the AmbientGAN approach. Training classifiers from noisy labels is a closely related problem. Recently, [34, 20] proposed a theoretically motivated classifier which minimizes the modified loss in presence of noisy labels and showed improvement over the robust classifiers [29, 45, 46].

Notation. For a vector x , $\|x\|_p = (\sum_i |x_i|^p)^{1/p}$ is the standard ℓ_p -norm. For a matrix A , let $\|A\|_p = \max_{\|x\|_p=1} \|Ax\|_p, \forall p \in \mathbb{N} \cup \{0, \infty\}$ denote the operator norm. Then $\|A\|_\infty = \max_i \sum_j |A_{ij}|$, $\|A\|_1 = \max_j \sum_i |A_{ij}|$ and $\|A\|_2 = \sigma_{\max}(A)$, the maximum singular value. $\mathbf{1}$ is all ones vector with appropriate dimensions and \mathbf{I} is identity matrix with appropriate dimensions. $[n] = \{1, 2, \dots, n\}, \forall n \geq 1$. For a vector $x \in \mathbb{R}^n$, x_i ($i \in [n]$) is its i -th coordinate.

2 Our first architecture: RCGAN

Training a conditional GAN with noisy samples results in a biased generator. We propose Robust Conditional GAN (RCGAN) architecture which has the following pre-processing, discriminator update, and generator update steps. We assume in this section that the confusions matrix C is known (and the marginal P_Y can easily be inferred), and address the case of unknown C in Section 4.

Pre-processing: We train a classifier h^* to predict the noisy label \tilde{y} given x under a loss l , trained on $h^* \in \arg \min_{h \in \mathcal{H}} \mathbb{E}_{(x, \tilde{y}) \sim \tilde{P}_{X, \tilde{Y}}} [\ell(h(x), \tilde{y})]$, where \mathcal{H} is a parametric family of classifiers (typically neural networks) and $\tilde{P}_{X, \tilde{Y}}$ is the joint distribution of real x and corresponding real noisy \tilde{y} .

D-step: We train on the following adversarial loss. In the second term below, y is generated according to P_Y and corresponding noisy labels are generated by corrupting the y according to the conditional distribution C_y which is the y -th row of the confusion matrix (assumed to be known):

$$\max_{D \in \mathcal{F}} \mathbb{E}_{(x, \tilde{y}) \sim \tilde{P}_{X, \tilde{Y}}} [\phi(D(x, \tilde{y}))] + \mathbb{E}_{\substack{z \sim N, y \sim P_Y \\ \tilde{y} \mid y \sim C_y}} [\phi(1 - D(G(z; y), \tilde{y}))],$$

where P_Y is the true marginal distribution of the labels, N is the distribution of the latent random vector, and \mathcal{F} is a family of discriminators.

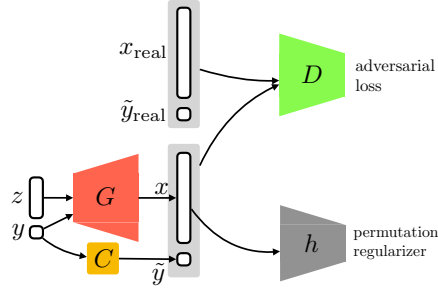


Figure 1: The output x of the conditional generator G is paired with a noisy label \tilde{y} corrupted by the channel C . The discriminator D estimates whether a given labeled sample is coming from the real data $(x_{\text{real}}, \tilde{y}_{\text{real}})$ or generated data (x, \tilde{y}) . The permutation regularizer h is pre-trained on real data.

G-step: We train on the following loss with some $\lambda > 0$:

$$\min_{G \in \mathcal{G}} \mathbb{E}_{\substack{z \sim N, y \sim P_Y \\ \tilde{y} | y \sim C_y}} [\phi(1 - D(G(z; y), \tilde{y})) + \lambda \ell(h^*(G(z; y)), y)] , \quad (2)$$

where \mathcal{G} is a family of generators. The idea of using auxiliary classifiers have been used to improve the quality of the image and stability of the training, for example in auxiliary classifier GAN (AC-GAN) [36], and improve the quality of clustering in the latent space [33]. We propose an auxiliary classifiers h , mitigating a *permutation error*, which we empirically identified on naive implementation of our idea with no regularizers.

Permutation regularizer (controlled by λ). Permutation error occurs if, when asked to produce samples from a target class, the trained generator produces samples dominantly from a single class but different from the target class. We propose a regularizer h^* , which predicts the *noisy* label \tilde{y} . As long as the confusion matrix is diagonally dominant, which is a necessary condition for identifiability, this regularizer encourages the correct permutation of the labels.

Theoretical motivation for RCGAN. When $\lambda = 0$, we get the standard conditional GAN update steps, albeit one which tries to minimize discriminator loss between the noisy real distribution \tilde{P} and the distribution \tilde{Q} of the generator when the label is passed through the same noisy channel parameterized by C . The main idea of RCGAN is to minimize a certain divergence between noisy real data and noisy generated data. For example, the choice of bounded functions $\mathcal{F} = \{D : \mathcal{X} \times [m] \rightarrow [0, 1]\}$ and identity map $\phi(a) = a$ leads to a total variation minimization; The loss minimized in the G-step is the total variation $d_{\text{TV}}(\tilde{P}, \tilde{Q}) \triangleq \sup_{S \in \mathcal{X} \times [m]} \{\tilde{P}(S) - \tilde{Q}(S)\}$ between the two distributions with corrupted labels, up to some scaling and some shift. If we choose $\mathcal{F} = \{D : \mathcal{X} \times [m] \rightarrow [0, 1]\}$ and $\phi(a) = \log(a)$, then we are minimizing the Jensen-Shannon divergence $d_{\text{JS}}(\tilde{P}, \tilde{Q}) \triangleq (1/2)d_{\text{KL}}(\tilde{P} \| (\tilde{P} + \tilde{Q})/2) + (1/2)d_{\text{KL}}(\tilde{Q} \| (\tilde{P} + \tilde{Q})/2)$, where $d_{\text{KL}}(\cdot \| \cdot)$ denotes the Kullback-Leibler divergence. The following theorem provides approximation guarantees for some common divergence measures over noisy channel, justifying our proposed practical approach. We refer to Appendix B for a proof.

Theorem 1. Let $P_{X,Y}$ and $Q_{X,Y}$ be two distributions on $\mathcal{X} \times [m]$. Let $\tilde{P}_{X,\tilde{Y}}, \tilde{Q}_{X,\tilde{Y}}$ be the corresponding distributions when samples from P, Q are passed through the noisy channel given by the confusion matrix $C \in \mathbb{R}^{m \times m}$ (as defined in Section 1). If C is full-rank, we get,

$$d_{\text{TV}}(\tilde{P}, \tilde{Q}) \leq d_{\text{TV}}(P, Q) \leq \|C^{-1}\|_{\infty} d_{\text{TV}}(\tilde{P}, \tilde{Q}) , \text{ and} \quad (3)$$

$$\frac{1}{8} d_{\text{JS}}(\tilde{P} \| \tilde{Q})^2 \leq d_{\text{JS}}(P \| Q) \leq \|C^{-1}\|_{\infty} \sqrt{8 d_{\text{JS}}(\tilde{P} \| \tilde{Q})} . \quad (4)$$

To interpret this theorem, let Q denote the distribution of the generator. The theorem implies that when the noisy generator distribution \tilde{Q} becomes close to the noisy real distribution \tilde{P} in total variation or in Jensen-Shannon divergence, then the generator distribution Q must be close to the distribution of real data P in the same metric. This justifies the use of the proposed architecture RCGAN. In practice, we minimize the sample divergence of the two distributions, instead of the population divergence as analyzed in the above theorem. However, these standard divergences are known to not generalize in training GANs [3]. To this end, we provide in Section 3 analyses on *neural network distances*, which are known to generalize, and provide finite sample bounds.

3 Theoretical Analysis of RCGAN

It was shown in [3] that standard GAN losses of Jensen-Shannon divergence and Wasserstein distance both fail to generalize with a finite number of samples. On the other hand, more recent advances in analyzing GANs in [56, 6, 4] show promising generalization bounds by either assuming Lipschitz conditions on the generator model or by restricting the analysis to certain classes of distributions. Under those assumptions, where JS divergence generalizes, Theorem 1 justifies the use of the proposed RCGAN. However, those require the distribution to be Gaussian, mixture of Gaussians, or output of a neural network generator, for example in [4].

In this section, we provide analyses of RCGAN on a distance that generalizes without any assumptions on the distribution of the real data as proven in [3]: *neural network distance*. Formally, consider a class of real-valued functions \mathcal{F} and a function $\phi : [0, 1] \rightarrow \mathbb{R}$ which is either convex or concave. The neural network distance is defined as

$$d_{\mathcal{F},\phi}(P, Q) \triangleq \sup_{D \in \mathcal{F}} \mathbb{E}_{(x,y) \sim P} [\phi(D(x, y))] + \mathbb{E}_{(x,y) \sim Q} [\phi(1 - D(x, y))] - \mu_\phi. \quad (5)$$

where P is the distribution of the real data, Q is that of the generated data, and μ_ϕ is the constant correction term to ensure that $d_{\mathcal{F},\phi}(P, P) = 0$. We further assume that \mathcal{F} includes three constant functions $D(x, y) = 0$, $D(x, y) = 1/2$, and $D(x, y) = 1$, in order to ensure that $d_{\mathcal{F},\phi}(P, Q) \geq 0$ and $d_{\mathcal{F},\phi}(P, P) = 0$, as shown in Lemma 1 in the Appendix.

The proposed RCGAN with $\lambda = 0$ approximately minimizes the neural network distance $d_{\mathcal{F},\phi}(\tilde{P}, \tilde{Q})$ between the two corrupted distributions. In practice, \mathcal{F} is a parametric family of functions from a specific neural network architecture that the designer has chosen. In theory, we aim to identify how the choice of class \mathcal{F} provides the desired approximation bounds similar to those in Theorem 1, but for neural network distances. This analysis leads to the choice of *projection discriminator* [32] to be used in RCGAN (Remark 2). On the other hand, we show in Theorem 3 that an inappropriate choice of the discriminator architecture can cause non-approximation. Further, we provide the sample complexity of the approximation bounds in Theorem 4.

We refer to the un-regularized version with $\lambda = 0$ as simply RCGAN. In this section, we focus on a class of loss functions called Integral Probability Metrics (IPM) where $\phi(x) = x$ [44]. This is a popular choice of loss in GANs in practice [47, 2, 8] and in analyses [4]. We write the induced neural network distance as $d_{\mathcal{F}}(P, Q)$, dropping the ϕ in the notation.

3.1 Approximation bounds for neural network distances

We define an operation \circ over a matrix $T \in \mathbb{R}^{m \times m}$ and a class \mathcal{F} of functions on $\mathcal{X} \times [m] \rightarrow \mathbb{R}$ as

$$T \circ \mathcal{F} \triangleq \left\{ f \in \mathcal{F} \mid f(x, y) = \sum_{\tilde{y} \in [m]} T_{y\tilde{y}} f(x, \tilde{y}) \right\}. \quad (6)$$

This makes it convenient to represent the neural network distance corrupted by noise with a confusion matrix $C \in \mathbb{R}^{m \times m}$, where $C_{y\tilde{y}}$ is the probability a label y is corrupted as \tilde{y} . Formally, it follows from (5) and (6) that $d_{\mathcal{F}}(\tilde{P}, \tilde{Q}) = d_{C \circ \mathcal{F}}(P, Q)$. We refer to Appendix E for a proof. For $d_{\mathcal{F}}(\tilde{P}, \tilde{Q})$ to be a good approximation of $d_{\mathcal{F}}(P, Q)$, we show that the following condition is sufficient.

Assumption 1. We assume that the class of discriminator functions \mathcal{F} can be decomposed into three parts $\mathcal{F} = \{f_1 + f_2 + c \mid f_1 \in \mathcal{F}_1, f_2 \in \mathcal{F}_2\}$ such that $c \in \mathbb{R}$ is any constant and

- \mathcal{F}_1 satisfies the inclusion condition:

$$T \circ \mathcal{F}_1 \subseteq \mathcal{F}_1, \quad (7)$$

for all $\|T\|_\infty \triangleq \max_i \sum_j |T_{ij}| = 1$; and

- \mathcal{F}_2 satisfies the label invariance condition: there exists a class $\mathcal{F}^{(x)}$ of sets of functions, parametrized by $x \in \mathcal{X}$, such that

$$\mathcal{F}_2 = \{\alpha f(x, y) \mid f(x, y) = f(x), f(x) \in \mathcal{F}^{(x)}, \alpha \in [0, 1]\}. \quad (8)$$

We discuss the necessity and practical implications of this assumption in Section 3.2, and give examples satisfying these assumptions in Remarks 2 and 3. Notice that a trivial class with a single constant zero function satisfies both inclusion and label invariance conditions. For example, we can choose $c = 0$ and also choose to set either $\mathcal{F}_1 = \{f(x, y) = 0\}$ or $\mathcal{F}_2 = \{f(x, y) = 0\}$, in which case \mathcal{F} only needs to satisfy either one of the conditions in Assumption 1. The flexibility that we gain by allowing the set addition $\mathcal{F}_1 + \mathcal{F}_2$ is critical in applying these conditions to practical discriminators, especially in proving Remark 2. Note that in the inclusion condition in Eq. 7, we require the condition to hold for all max-norm bounded set: $\{T : \max_i \sum_j |T_{ij}| = 1\}$. The reason a weaker condition of all row-stochastic matrices, $\{T : \sum_j T_{ij} = 1\}$, does not suffice is that in order to prove the upper bound in Eq. 9, we need to apply the invariance condition to $\|C^{-1}\|_\infty^{-1} C^{-1} \circ \mathcal{F}$. This matrix $\|C^{-1}\|_\infty^{-1} C^{-1}$ is not row-stochastic, but still max-norm bounded.

We first show that Assumption 1 is sufficient for approximability of the neural network distance from corrupted samples. For two distributions $P_{X,Y}$ and $Q_{X,Y}$ on $\mathcal{X} \times [m]$, let $\tilde{P}_{X,\tilde{Y}}$ and $\tilde{Q}_{X,\tilde{Y}}$ be the corresponding corrupted distributions respectively, where the label Y is passed through the noisy channel defined by the confusion matrix $C \in \mathbb{R}^{m \times m}$, i.e. $\tilde{P}(x, \tilde{y}) = \sum_y P(x, y) C_{y, \tilde{y}}$.

Theorem 2. If a class of functions \mathcal{F} satisfies Assumption 1, then

$$d_{\mathcal{F}}(\tilde{P}, \tilde{Q}) \leq d_{\mathcal{F}}(P, Q) \leq \|C^{-1}\|_\infty d_{\mathcal{F}}(\tilde{P}, \tilde{Q}), \quad (9)$$

where we follow the convention that $\|C^{-1}\|_\infty = \infty$ if C is not full rank.

We refer to Appendix E for a proof. This gives a sharp characterization on how two distances are related: the one we can minimize in training RCGAN (i.e. $d_{\mathcal{F}}(\tilde{P}, \tilde{Q})$) and the true measure of closeness (i.e. $d_{\mathcal{F}}(P, Q)$). Although the latter cannot be directly evaluated or minimized, RCGAN is approximately minimizing the true neural network distance $d_{\mathcal{F}}(P, Q)$ as desired.

The lower bound proves a special case of the data-processing inequality. Two random variables from P and Q get closer in neural network distance, when passed through a stochastic transformation. The upper bound puts a limit on how much closer \tilde{P} and \tilde{Q} can get, depending on the noise level. This fundamental trade-off is captured by $\|C^{-1}\|_\infty$. Under the noiseless case where C is the identity matrix, we have $\|C^{-1}\|_\infty = 1$ and we recover a trivial fact that the two distances are equal. On the other extreme, if C is rank deficient, we use the convention that $\|C^{-1}\|_\infty = \infty$ and the two distances can be arbitrarily different. The approximation factor of $\|C^{-1}\|_\infty$ captures how much the space \mathcal{F} can shrink by the noise C . This coincides with Theorem 1, where a similar trade-off was identified for the TV distance. Next remark shows that these bounds cannot be tightened for general P , Q , and \mathcal{F} . A proof is provided in Appendix D.

Remark 1. For any full-rank confusion matrix $C \in \mathbb{R}^{d_1 \times d_2}$, there exist pairs of distributions (P_1, Q_1) and (P_2, Q_2) , and a function class \mathcal{F} satisfying Assumption 1, such that

1. $d_{\mathcal{F}}(\tilde{P}_1, \tilde{Q}_1) = d_{\mathcal{F}}(P_1, Q_1)$, and

$$2. \ d_{\mathcal{F}}(P_2, Q_2) = \|C^{-1}\|_{\infty} d_{\mathcal{F}}(\tilde{P}_2, \tilde{Q}_2).$$

Theorem 2 shows that (i) RCGAN can learn the true conditional distribution, justifying its use; and (ii) performance of RCGAN is determined by how noisy the samples are via $\|C^{-1}\|_{\infty}$. There are still two loose ends. First, does practical implementation of RCGAN architecture satisfy the inclusion and/or label invariance assumptions? Secondly, in practice we cannot minimize $d_{\mathcal{F}}(\tilde{P}, \tilde{Q})$ as we only have a finite number of samples. How much do we lose in this finite sample regime? We give precise answers to each question in the following two sections.

3.2 Inclusion and label invariance assumptions

Several class of functions satisfy Assumption 1 (c.f. Remark 3). For RCGAN, we propose a popular state-of-the-art discriminator for conditional GANs known as the *projection discriminator* [32], parametrized by $V \in \mathbb{R}^{m \times d_V}$, $v \in \mathbb{R}^{d_v}$, and $\theta \in \mathbb{R}^{d_{\theta}}$:

$$D_{V,v,\theta}(x, y) = \text{vec}(y)^T V \psi(x; \theta) + v^T \psi'(x; \theta), \quad (10)$$

where $\psi(x; \theta) \in \mathbb{R}^{d_V}$ and $\psi'(x; \theta) \in \mathbb{R}^{d_v}$ are vector valued parametric functions for some integers d_V , d_v , and $\text{vec}(y)^T = [\mathbb{I}_{y=1}, \dots, \mathbb{I}_{y=m}]$. The first term satisfies the inclusion condition, as any operation with T can be absorbed into V . The second term is label invariant as it does not depend on y . This is made precise in the following remark, whose proof is provided in Appendix F. Together with this remark, the approximability result in Theorem 2 justifies the use of projection discriminators in RCGAN, which we use in all our experiments.

Remark 2. *The class of projection discriminators $\{D_{V,v,\theta}(x, y)\}_{V \in \mathcal{V}_1, v \in \mathcal{V}_2, \theta \in \Theta}$ defined in Eq. 10 satisfies Assumption 1 for any ψ , ψ' , and Θ , if $\mathcal{V}_1 = \{V \in \mathbb{R}^{m \times d_V} \mid \max_i |V_{ij}| \leq 1 \text{ for all } j \in [d_V]\}$, and $\mathcal{V}_2 = \{v \in \mathbb{R}^{d_v} \mid \|v\| \leq 1\}$.*

Other choices of \mathcal{V}_1 and \mathcal{V}_2 are also possible. For example, $\mathcal{V}'_1 = \{V \in \mathbb{R}^{m \times d_V} \mid \sum_j \max_i |V_{ij}| \leq 1\}$ or $\mathcal{V}''_1 = \{V \in \mathbb{R}^{m \times d_V} \mid \|V\|_{\infty} = \max_i \sum_j |V_{ij}| \leq 1\}$ are also sufficient. We find the proposed choice of \mathcal{V}_1 easy to implement, as a column-wise L_{∞} -norm normalization via projected gradient descent. We describe implementation details in Appendix I.

Next, we ask if Assumption 1 is necessary also. We show that for all pairs of distributions (P, Q) satisfying the following technical conditions, and all confusion matrix C , there exists a class \mathcal{F} where approximation bounds in (9) fail.

Assumption 2. *We consider a pair of distributions $P_{X,Y}$ and $Q_{X,Y}$ and a confusion matrix C satisfying the following conditions:*

- *The random variable X conditioned on $Y = y$ is a continuous random variable with density functions $dP_{X|Y=y}$ and $dQ_{X|Y=y}$, respectively.*
- *There exists $S \subseteq \mathcal{X}$ such that $P_X(S) + Q_X(S) > 0$, and $P_{X,Y}(x, \cdot) - Q_{X,Y}(x, \cdot)$ is not a right eigenvector of C , for all $x \in S$, where $P_{X,Y}(x, \cdot) = [P_{X,Y}(x, 1), \dots, P_{X,Y}(x, m)]^T$.*

A pair (P, Q) violating the above assumptions either has X that is a mixture of continuous and discrete distribution, or all $(P(x, \cdot) - Q(x, \cdot))$'s are aligned with the right eigenvectors of C .

Theorem 3. *For all sufficiently small $\epsilon > 0$, all distributions $P_{X,Y}$ and $Q_{X,Y}$ satisfying Assumption 2, and all full-rank $C \in \mathbb{R}^{m \times m}$, there exist \mathcal{F}_3 not satisfying Assumption 1, such that*

$$d_{\mathcal{F}_3}(\tilde{P}, \tilde{Q}) \leq O_{\epsilon}(\epsilon) \quad \text{and} \quad d_{\mathcal{F}_3}(P, Q) \geq O_{\epsilon}(1), \quad (11)$$

and \mathcal{F}_4 not satisfying Assumption 1, such that

$$d_{\mathcal{F}_4}(\tilde{P}, \tilde{Q}) \geq O_{\epsilon}(1) \quad \text{and} \quad d_{\mathcal{F}_4}(P, Q) \leq O_{\epsilon}(\epsilon). \quad (12)$$

We refer to Appendix G for a proof. This implies that some assumptions on the function class \mathcal{F} are necessary, such as those in Assumption 1. Without any restrictions, we can find bad examples where the two distances $d_{\mathcal{F}}(P, Q)$ and $d_{\mathcal{F}}(\tilde{P}, \tilde{Q})$ are arbitrarily different for any C , $P_{X,Y}$, and $Q_{X,Y}$.

3.3 Finite sample analysis

In practice, we do not have access to the probability distributions \tilde{P} and \tilde{Q} . Instead, we observe a set of samples of a finite size n , from each of them. In training GAN, we minimize the *empirical* neural network distance, $d_{\mathcal{F}}(\tilde{P}_n, \tilde{Q}_n)$, where \tilde{P}_n and \tilde{Q}_n denote the empirical distribution of n samples. Inspired from the recent generalization results in [3], we show that this empirical distance minimization leads to small $d_{\mathcal{F}}(P, Q)$ up to an additive error that vanishes with an increasing sample size. As shown in [3], Lipschitz and bounded function classes are critical in achieving sample efficiency for GANs. We follow the same approach over a similar function class. Let

$$\mathcal{F}_{p,L} = \{D_u(x, y) \in [0, 1] \mid D_u(x, y) \text{ is } L\text{-Lipschitz in } u \text{ and } u \in \mathcal{U} \subseteq \mathbb{R}^p\}, \quad (13)$$

be a class of bounded functions with parameter $u \in \mathbb{R}^p$. We say that \mathcal{F} is L -Lipschitz in u if

$$|D_{u_1}(x, y) - D_{u_2}(x, y)| \leq L\|u_1 - u_2\|, \quad \forall u_1, u_2 \in \mathcal{U}, x \in \mathcal{X}, y \in [m]. \quad (14)$$

Theorem 4. *For any class $\mathcal{F}_{p,L}$ of bounded Lipschitz functions $D_u(x, y)$ satisfying Assumption 1, there exists a universal constant $c > 0$ such that*

$$d_{\mathcal{F}_{p,L}}(\tilde{P}_n, \tilde{Q}_n) - \epsilon \leq d_{\mathcal{F}_{p,L}}(P, Q) \leq \|C^{-1}\|_{\infty} (d_{\mathcal{F}_{p,L}}(\tilde{P}_n, \tilde{Q}_n) + \epsilon), \quad (15)$$

with probability at least $1 - e^{-p}$ for any $\epsilon > 0$ and n large enough, $n \geq (cp/\epsilon^2) \log(pL/\epsilon)$.

We refer to Appendix H for a proof. This justifies the use of the proposed RCGAN which minimizes $d_{\mathcal{F}}(\tilde{P}_n, \tilde{Q}_n)$, as it leads to the generator Q being close to the real distribution P in neural network distance, $d_{\mathcal{F}}(P, Q)$. These bounds inherit the approximability of the population version in Theorem 2.

4 Our second architecture: RCGAN-U

In many real world scenarios the confusion matrix C is unknown. We propose RCGAN-Unknown (RCGAN-U) algorithm which jointly estimates the real distribution P and the noise model C . The pre-processing and D steps of the RCGAN-U are the same as those of RCGAN, assuming the current guess M of the confusion matrix. As the G-step in (2) is not differentiable in C , we use the following reparameterized estimator of the loss, motivated by similar technique in training classifiers from noisy labels:

$$\min_{G \in \mathcal{G}, M \in \mathcal{C}} \mathbb{E}_{z \sim N, y \sim P_Y} [\phi_M(G(z; y), y, D) + \lambda l(h^*(G(z; y)), y)]$$

where \mathcal{C} is the set of all transition matrices and $\phi_M(x, y, D) = \sum_{\tilde{y} \in [m]} M_{y\tilde{y}} \phi(1 - D(x, \tilde{y}))$.

5 Experiments

Implementation details are explained in Appendix I. We consider one-coin based models, which are parameterized by their label accuracy probability α . In this model a sample with true label y is flipped uniformly at random to label \tilde{y} in $[m] \setminus \{y\}$ with probability $1 - \alpha$. The entries of its confusion matrix C , will then be $C_{ii} = \alpha$ and $C_{i \neq j} = (1 - \alpha)/(m - 1)$, where m is the number of classes. We call this model *uniform flipping* model. We train proposed GANs on MNIST and CIFAR-10 datasets [25, 24] and compare them to two baselines. Code to reproduce our experiments is available at <https://github.com/POLane16/Robust-Conditional-GAN>.

Baselines. First is the *biased GAN*, which is a conditional GAN applied directly on the noisy data. The loss is hence biased, and the true conditional distribution is not the optimal solution of this biased loss. Next natural baseline is using de-biased classifier as the discriminator, motivated by the approach of [34] on learning classifiers from noisy labels. The main insight is to modify the loss function according to C , such that in expectation the loss matches that of the clean data. We refer to this approach as *unbiased GAN*. Concretely, when training the discriminator, we propose the following (modified) de-biased loss:

$$\max_{D \in \mathcal{F}} \mathbb{E}_{(x, \tilde{y}) \sim \tilde{P}_{X, \tilde{Y}}} \left[\sum_{y \in [m]} (C^{-1})_{\tilde{y}y} \phi(D(x, y)) \right] + \mathbb{E}_{z \sim N} \mathbb{E}_{y \sim P_Y} [\phi(1 - D(G(z; y), y))]. \quad (16)$$

This is unbiased, as the first term is equivalent to $\mathbb{E}_{(x, y) \sim P_{X, Y}} [\phi(D(x, y))]$, which is the standard GAN loss with clean samples. However, such de-biasing is sensitive to the condition number of C , and can become numerically unstable for noisy channels as C^{-1} has large entries [20]. For both the dataset, we use linear classifiers for permutation regularizer of the RCGAN-U architecture.

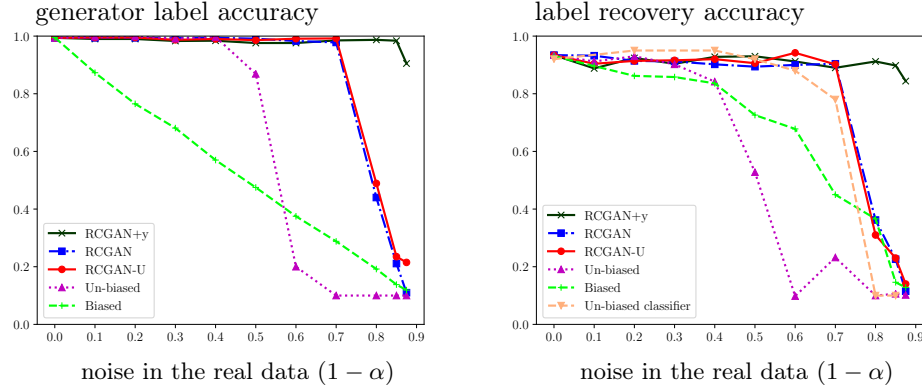


Figure 2: Noisy MNIST dataset: Our RCGAN models consistently improves upon all competing baseline approaches in generator label accuracy (left). The trend continues in label recovery accuracy (right), where our proposed RCGAN-classifiers improves upon *unbiased classifier* [34], which is one of the state-of-the-art approaches tailored for label recovery. The numerical values of the data points are given in a table in Appendix J.

5.1 MNIST

We train five architectures on MNIST dataset corrupted by the uniform flipping noise: RCGAN+y, RCGAN, RCGAN-U, unbiased GAN, and biased GAN. RCGAN+y architecture has the same architecture as RCGAN but the input to the first layer of its discriminator is concatenated with a one-hot representation of the label. We discuss our techniques to overcome the challenges involved in training RCGAN+y in Appendix I.

Conditional generators can be used to generate samples x from a particular class y , in the classes it learned. We then can use a pre-trained classifier f to compare y to the true class of the sample, $f(x)$ (as perceived by the classifier f). We compare the *generator label accuracy* defined as $\mathbb{E}_{y \sim P_Y, Z \sim N} [\mathbb{I}_{\{y=f(G(z, y))\}}]$, in Figure 2, left panel. We generated 10k labels chosen uniformly at random and corresponding conditional samples from the generators, and calculated the generator label accuracy using a CNN classifier pre-trained on the clean MNIST data to an accuracy of 99.2%. The proposed RCGAN significantly improves upon the competing baselines, and achieves almost perfect label accuracy until a high noise of $\alpha = 0.3$. RCGAN+y further improves upon RCGAN and to gain very high accuracy even at $\alpha = 0.125$. The high accuracy of RCGAN-U suggests that robust training is possible without prior knowledge of the confusion matrix C . As expected, biased GAN has an accuracy of approximately $1 - \alpha$.

An immediate application of robust GANs is recovering the true labels of the noisy training data, which is an important and challenging problem in crowdsourcing. We propose a new meta-algorithm, which we call cGAN-label-recovery, which uses any conditional generator $G(z, y)$ trained on the noisy samples, to estimate the true label, as \hat{y} , of a sample x using the following optimization.

$$\hat{y} \in \arg \min_{y \in [m]} \left\{ \min_{z_y} \|G(z_y, y) - x\|_2^2 \right\}. \quad (17)$$

In the right panel of Figure 2 we compare the *label recovery accuracy* of the meta-algorithm using the five conditional GANs, on 500 randomly chosen noisy training samples. This is also compared to a state-of-the-art method [34] for label recovery, which proposed minimizing unbiased loss function given the noisy labels and the confusion matrix. This unbiased classifier, was shown to outperforms the robust classifiers [29, 45, 46] and can be used to predict the true label of the training examples. In Figures 4 of Appendix J, we show example images from all the generators.

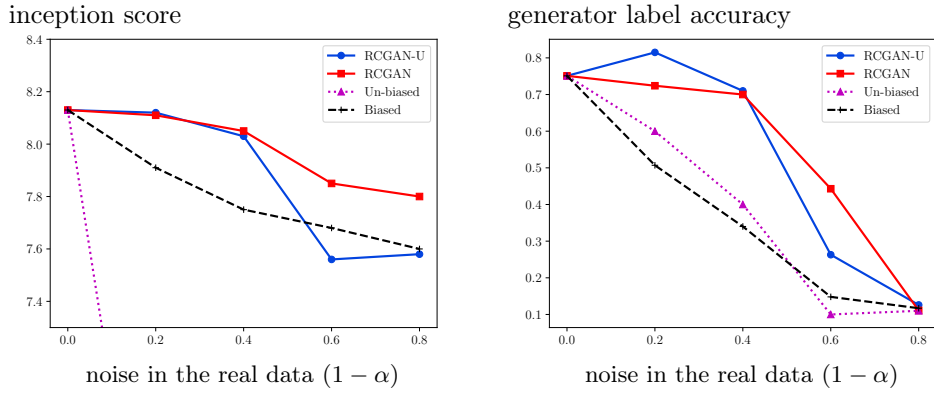


Figure 3: Noisy CIFAR-10 dataset: Our RCGAN (red) and RCGAN-U (blue) consistently improves upon Unbiased (magenta) and Biased (black) GANs trained on noisy CIFAR-10 in inception scores (left) and in generator label accuracy (right). The numerical values of the data points are given in a table in Appendix J.

5.2 CIFAR-10

In Figure 3, we show the inception score [40] and the label accuracy of the conditional generator for the four approaches: our proposed RCGAN and RCGAN-U, against the baselines Unbiased (Section 5) and Biased (Section 1) GANs trained using CIFAR-10 images [24], while varying the label accuracy of the real data under uniform flipping. In RCGAN-U, even with the regularizer, the learned confusion matrix was a permuted version of the true C , possibly because a linear classifier might be too simple to classify CIFAR images. To combat this, we initialized the confusion matrix M to be diagonally dominant (Appendix I).

In the left panel of Figure 3, our RCGAN and RCGAN-U consistently achieve higher inception scores than the other two approaches. The Unbiased GAN is highly unstable and hence produces garbage images for large noise (Fig. 5), possibly due to numerical instability of $\|C^{-1}\|_\infty$, as noted in [20]. This confirms that robust GANs not only produce images from the correct class, but also produce better quality images. In the right panel of Figure 3, we report the generator label accuracy (Section 5.1) on 1k samples generated by each GAN. We classify the generator images using a ResNet-110 model trained to an accuracy of 92.3% on the noiseless CIFAR-10 dataset¹. Biased GAN has significantly lower label accuracy whereas the Unbiased GAN has low inception score. In Figure 5 in Appendix J, we show example images from the three generators for the different flipping probabilities. We believe that the gain in using the proposed robust GANs will be

¹<https://github.com/wenxinwu/resnet-in-tensorflow>

larger, when we train to higher accuracy with larger networks and extensive hyper parameter tuning, with latest innovations in GAN architectures, for example [54, 28, 17, 19, 41].

6 Numerical comparisons with AmbientGAN [10]

In Table 1, we plot the generated label accuracy (as defined in Section 5.1) of RCGAN (which uses the proposed projection discriminator) and AmbientGAN (which uses the DCGAN with no projection discriminator) for multiple values of noise levels ($1 - \alpha$). One of the main reasons for the performance drop of AmbientGAN is that without the projection discriminator, training of AmbientGAN is sensitive to how the mini-batches are chosen. For example, if the distribution of the labels in the mini-batch of the real data is different from that of the mini-batch of the generated data, then the performance of (conditional) AmbientGAN significantly drops. This is critical as we have noisy labels, and matching the labels is in the mini-batch is challenging. Our proposed RCGAN provides an architecture and training methods for applying AmbientGAN to noisy labeled data, to overcome these challenges. When a projection discriminator is used, as in all our RCGAN and RCGAN-U implementations, the performance is not sensitive to how the mini-batches are sampled. When a discriminator that is not necessarily a projection discriminator is used, as in our RCGAN+ y architecture, we propose a novel scheduling of the training, which avoids local minima resulting from mis-matched mini-batches (explained in Appendix I). The results are averaged over 10 instances.

	Noise level ($1 - \alpha$)		
	0.2	0.3	0.5
RCGAN	0.994	0.994	0.994
AmbientGAN	0.940	0.902	0.857

Table 1: Noisy MNIST dataset: in generated label accuracy, RCGAN improves upon the standard implementation of the AmbientGAN with DCGAN architecture (we refer to Appendix I for implementation details)

7 Conclusion

Standard conditional GANs can be sensitive to noise in the labels of the training data. We propose two new architectures to make them robust, one requiring the knowledge of the distribution of the noise and another which does not, and demonstrate the robustness on benchmark datasets of CIFAR-10 and MNIST. We further showcase how the learned generator can be used to recover the corrupted labels in the training data, which can potentially be used in practical applications. The proposed architecture combines the noise adding idea of AmbientGAN [10], projection discriminator of [32], and regularizers similar to those in InfoGAN [11]. Inspired by AmbientGAN [10], the main idea is to pair the generator output image with a label that is passed through a noisy channel, before feeding to the discriminator. We justify this idea of noise adding by identifying a certain class of discriminators that have good generalization properties. In particular, we prove that projection discriminator, introduced in [32], has a good generalization property. We showcase that the proposed architecture, when trained with a regularizer, has superior robustness on benchmark datasets.

One weakness of our theoretical result in Theorem 4 is that depending on the choice of $\mathcal{F}_{p,L}$ (i.e. the representation power of the parametric class $D_u(x, y)$), closeness in the neural network distance does not always imply closeness of the distributions. It is generally a challenging problem to address generalization for specific function class \mathcal{F} and a pair of distributions P and Q . However, a recent breakthrough in generalization properties of GAN in [4] makes the connection between $d_{\mathcal{F}}(\tilde{P}_n, \tilde{Q}_n)$ and $d_{\text{TV}}(P, Q)$ precise, under some assumptions on the P and Q . This leads to the following research question: under which class of distributions P and Q does the neural network distance of the proposed conditional GAN with projection discriminator

generalize? The emphasis is in studying the class of functions satisfying Assumption 1 and identifying corresponding family of distributions that generalize under this function class.

Acknowledgement

This work is supported by NSF awards CNS-1527754, CCF-1553452, CCF-1705007, RI-1815535 and Google Faculty Research Award. This work used the Extreme Science and Engineering Discovery Environment (XSEDE), which is supported by National Science Foundation grant number OCI-1053575. Specifically, it used the Bridges system, which is supported by NSF award number ACI-1445606, at the Pittsburgh Supercomputing Center (PSC). This work is partially supported by the generous research credits on AWS cloud computing resources from Amazon.

References

- [1] Panos Achlioptas, Olga Diamanti, Ioannis Mitliagkas, and Leonidas Guibas. Representation learning and adversarial generation of 3d point clouds. *arXiv preprint arXiv:1707.02392*, 2017.
- [2] Martin Arjovsky, Soumith Chintala, and Léon Bottou. Wasserstein gan. *arXiv preprint arXiv:1701.07875*, 2017.
- [3] Sanjeev Arora, Rong Ge, Yingyu Liang, Tengyu Ma, and Yi Zhang. Generalization and equilibrium in generative adversarial nets (gans). *arXiv preprint arXiv:1703.00573*, 2017.
- [4] Yu Bai, Tengyu Ma, and Andrej Risteski. Approximability of discriminators implies diversity in GANs. *arXiv preprint arXiv:1806.10586*, 2018.
- [5] David Berthelot, Tom Schumm, and Luke Metz. Began: Boundary equilibrium generative adversarial networks. *arXiv preprint arXiv:1703.10717*, 2017.
- [6] G Biau, B Cadre, M Sangnier, and U Tanielian. Some theoretical properties of GANs. *arXiv preprint arXiv:1803.07819*, 2018.
- [7] Battista Biggio, Blaine Nelson, and Pavel Laskov. Support vector machines under adversarial label noise. In *Asian Conference on Machine Learning*, pages 97–112, 2011.
- [8] Mikołaj Bińkowski, Dougal J Sutherland, Michael Arbel, and Arthur Gretton. Demystifying MMD GANs. *arXiv preprint arXiv:1801.01401*, 2018.
- [9] Ashish Bora, Ajil Jalal, Eric Price, and Alexandros G Dimakis. Compressed sensing using generative models. *arXiv preprint arXiv:1703.03208*, 2017.
- [10] Ashish Bora, Eric Price, and Alexandros G Dimakis. Ambientgan: Generative models from lossy measurements. In *International Conference on Learning Representations (ICLR)*, 2018.
- [11] Xi Chen, Yan Duan, Rein Houthooft, John Schulman, Ilya Sutskever, and Pieter Abbeel. InfoGAN: Interpretable representation learning by information maximizing generative adversarial nets. In *Advances in Neural Information Processing Systems*, pages 2172–2180, 2016.
- [12] Alexander Philip Dawid and Allan M Skene. Maximum likelihood estimation of observer error-rates using the em algorithm. *Applied statistics*, pages 20–28, 1979.
- [13] Emily L Denton, Soumith Chintala, Rob Fergus, et al. Deep generative image models using a Laplacian pyramid of adversarial networks. In *Advances in neural information processing systems*, pages 1486–1494, 2015.

- [14] Ian Goodfellow, Jean Pouget-Abadie, Mehdi Mirza, Bing Xu, David Warde-Farley, Sherjil Ozair, Aaron Courville, and Yoshua Bengio. Generative adversarial nets. In *Advances in neural information processing systems*, pages 2672–2680, 2014.
- [15] Ishaan Gulrajani, Faruk Ahmed, Martin Arjovsky, Vincent Dumoulin, and Aaron C Courville. Improved training of wasserstein gans. In *Advances in Neural Information Processing Systems*, pages 5769–5779, 2017.
- [16] Phillip Isola, Jun-Yan Zhu, Tinghui Zhou, and Alexei A Efros. Image-to-image translation with conditional adversarial networks. *arXiv preprint*, 2017.
- [17] Alexia Jolicoeur-Martineau. The relativistic discriminator: a key element missing from standard GAN. *arXiv preprint arXiv:1807.00734*, 2018.
- [18] David R Karger, Sewoong Oh, and Devavrat Shah. Iterative learning for reliable crowdsourcing systems. In *Advances in neural information processing systems*, pages 1953–1961, 2011.
- [19] Tero Karras, Timo Aila, Samuli Laine, and Jaakko Lehtinen. Progressive growing of GANs for improved quality, stability, and variation. *arXiv preprint arXiv:1710.10196*, 2017.
- [20] Ashish Khetan, Zachary C Lipton, and Anima Anandkumar. Learning from noisy singly-labeled data. *arXiv preprint arXiv:1712.04577*, 2017.
- [21] Taeksoo Kim, Moonsu Cha, Hyunsoo Kim, Jungkwon Lee, and Jiwon Kim. Learning to discover cross-domain relations with generative adversarial networks. *arXiv preprint arXiv:1703.05192*, 2017.
- [22] Diederik P Kingma and Max Welling. Auto-encoding variational bayes. *arXiv preprint arXiv:1312.6114*, 2013.
- [23] Murat Kocaoglu, Christopher Snyder, Alexandros G Dimakis, and Sriram Vishwanath. Causalgan: Learning causal implicit generative models with adversarial training. *arXiv preprint arXiv:1709.02023*, 2017.
- [24] Alex Krizhevsky and Geoffrey Hinton. Learning multiple layers of features from tiny images. Technical report, Citeseer, 2009.
- [25] Yann LeCun. The mnist database of handwritten digits. <http://yann.lecun.com/exdb/mnist/>, 1998.
- [26] Christian Ledig, Lucas Theis, Ferenc Huszár, Jose Caballero, Andrew Cunningham, Alejandro Acosta, Andrew Aitken, Alykhan Tejani, Johannes Totz, Zehan Wang, et al. Photo-realistic single image super-resolution using a generative adversarial network. *arXiv preprint*, 2016.
- [27] Xiaodan Liang, Lisa Lee, Wei Dai, and Eric P Xing. Dual motion gan for future-flow embedded video prediction. *arXiv preprint*, 2017.
- [28] Zinan Lin, Ashish Khetan, Giulia Fanti, and Sewoong Oh. PacGAN: The power of two samples in generative adversarial networks. *arXiv preprint arXiv:1712.04086*, 2017.
- [29] Bing Liu, Yang Dai, Xiaoli Li, Wee Sun Lee, and Philip S Yu. Building text classifiers using positive and unlabeled examples. In *Data Mining, 2003. ICDM 2003. Third IEEE International Conference on*, pages 179–186. IEEE, 2003.
- [30] Mehdi Mirza and Simon Osindero. Conditional generative adversarial nets. *arXiv preprint arXiv:1411.1784*, 2014.
- [31] Takeru Miyato, Toshiki Kataoka, Masanori Koyama, and Yuichi Yoshida. Spectral normalization for generative adversarial networks. *arXiv preprint arXiv:1802.05957*, 2018.

- [32] Takeru Miyato and Masanori Koyama. cGANs with projection discriminator. *arXiv preprint arXiv:1802.05637*, 2018.
- [33] Sudipto Mukherjee, Himanshu Asnani, Eugene Lin, and Sreeram Kannan. Clustergan: Latent space clustering in generative adversarial networks. *arXiv preprint arXiv:1809.03627*, 2018.
- [34] Nagarajan Natarajan, Inderjit S Dhillon, Pradeep K Ravikumar, and Ambuj Tewari. Learning with noisy labels. In *Advances in neural information processing systems*, pages 1196–1204, 2013.
- [35] Anh Nguyen, Jason Yosinski, Yoshua Bengio, Alexey Dosovitskiy, and Jeff Clune. Plug & play generative networks: Conditional iterative generation of images in latent space. *arXiv preprint arXiv:1612.00005*, 2016.
- [36] Augustus Odena, Christopher Olah, and Jonathon Shlens. Conditional image synthesis with auxiliary classifier gans. *arXiv preprint arXiv:1610.09585*, 2016.
- [37] Alec Radford, Luke Metz, and Soumith Chintala. Unsupervised representation learning with deep convolutional generative adversarial networks. *arXiv preprint arXiv:1511.06434*, 2015.
- [38] Scott Reed, Zeynep Akata, Xinchen Yan, Lajanugen Logeswaran, Bernt Schiele, and Honglak Lee. Generative adversarial text to image synthesis. *arXiv preprint arXiv:1605.05396*, 2016.
- [39] Olga Russakovsky, Jia Deng, Hao Su, Jonathan Krause, Sanjeev Satheesh, Sean Ma, Zhiheng Huang, Andrej Karpathy, Aditya Khosla, Michael Bernstein, et al. Imagenet large scale visual recognition challenge. *International Journal of Computer Vision*, 115(3):211–252, 2015.
- [40] Tim Salimans, Ian Goodfellow, Wojciech Zaremba, Vicki Cheung, Alec Radford, and Xi Chen. Improved techniques for training gans. In *Advances in Neural Information Processing Systems*, pages 2234–2242, 2016.
- [41] Maziar Sanjabi, Jimmy Ba, Meisam Razaviyayn, and Jason D Lee. Solving approximate Wasserstein GANs to stationarity. *arXiv preprint arXiv:1802.08249*, 2018.
- [42] Rajat Sen, Karthikeyan Shanmugam, Himanshu Asnani, Arman Rahimzamani, and Sreeram Kannan. Mimic and classify: A meta-algorithm for conditional independence testing. *arXiv preprint arXiv:1806.09708*, 2018.
- [43] Ashish Shrivastava, Tomas Pfister, Oncel Tuzel, Josh Susskind, Wenda Wang, and Russ Webb. Learning from simulated and unsupervised images through adversarial training. In *The IEEE Conference on Computer Vision and Pattern Recognition (CVPR)*, volume 3, page 6, 2017.
- [44] Bharath K Sriperumbudur, Kenji Fukumizu, Arthur Gretton, Bernhard Schölkopf, and Gert RG Lanckriet. On integral probability metrics, ϕ -divergences and binary classification. *arXiv preprint arXiv:0901.2698*, 2009.
- [45] Guillaume Stempfel and Liva Ralaivola. Learning kernel perceptrons on noisy data using random projections. In *International Conference on Algorithmic Learning Theory*, pages 328–342. Springer, 2007.
- [46] Guillaume Stempfel and Liva Ralaivola. Learning svms from sloppily labeled data. In *International Conference on Artificial Neural Networks*, pages 884–893. Springer, 2009.
- [47] Dougal J Sutherland, Hsiao-Yu Tung, Heiko Strathmann, Soumyajit De, Aaditya Ramdas, Alex Smola, and Arthur Gretton. Generative models and model criticism via optimized maximum mean discrepancy. *arXiv preprint arXiv:1611.04488*, 2016.
- [48] Aaron van den Oord, Nal Kalchbrenner, and Koray Kavukcuoglu. Pixel recurrent neural networks. *arXiv preprint arXiv:1601.06759*, 2016.

- [49] David Van Veen, Ajil Jalal, Eric Price, Sriram Vishwanath, and Alexandros G Dimakis. Compressed sensing with deep image prior and learned regularization. *arXiv preprint arXiv:1806.06438*, 2018.
- [50] Carl Vondrick, Hamed Pirsiavash, and Antonio Torralba. Generating videos with scene dynamics. In *Advances In Neural Information Processing Systems*, pages 613–621, 2016.
- [51] Jiajun Wu, Chengkai Zhang, Tianfan Xue, Bill Freeman, and Josh Tenenbaum. Learning a probabilistic latent space of object shapes via 3d generative-adversarial modeling. In *Advances in Neural Information Processing Systems*, pages 82–90, 2016.
- [52] Zhi Xu, Chengtao Li, and Stefanie Jegelka. Robust gans against dishonest adversaries. *arXiv preprint arXiv:1802.09700*, 2018.
- [53] Raymond Yeh, Chen Chen, Teck Yian Lim, Mark Hasegawa-Johnson, and Minh N Do. Semantic image inpainting with perceptual and contextual losses. *arXiv preprint arXiv:1607.07539*, 2016.
- [54] Han Zhang, Ian Goodfellow, Dimitris Metaxas, and Augustus Odena. Self-attention generative adversarial networks. *arXiv preprint arXiv:1805.08318*, 2018.
- [55] Han Zhang, Tao Xu, Hongsheng Li, Shaoting Zhang, Xiaolei Huang, Xiaogang Wang, and Dimitris Metaxas. Stackgan: Text to photo-realistic image synthesis with stacked generative adversarial networks. In *IEEE Int. Conf. Comput. Vision (ICCV)*, pages 5907–5915, 2017.
- [56] Pengchuan Zhang, Qiang Liu, Dengyong Zhou, Tao Xu, and Xiaodong He. On the discrimination-generalization tradeoff in GANs. *arXiv preprint arXiv:1711.02771*, 2017.
- [57] Jun-Yan Zhu, Philipp Krähenbühl, Eli Shechtman, and Alexei A Efros. Generative visual manipulation on the natural image manifold. In *European Conference on Computer Vision*, pages 597–613. Springer, 2016.
- [58] Jun-Yan Zhu, Taesung Park, Phillip Isola, and Alexei A Efros. Unpaired image-to-image translation using cycle-consistent adversarial networks. *arXiv preprint arXiv:1703.10593*, 2017.

Appendix

A Notations and Lemmas

A.1 Additional Notation

Here we define some additional notations required for the proof. We define certain notations before we provide the main theoretical contributions of our paper. If $f(x, y)$ is a function of two variable of x, y , where $y \in [m]$, then $\bar{f}(x)$ is the vector $[f(x, 1), \dots, f(x, m)]^T$. If $P_{X,Y}$ is probability distribution of $(X, Y) \in \mathcal{X} \times [m]$, then $P_{Y|X=x}$ is the conditional distribution of Y given $X = x$.

For a matrix A , let $\|A\|_p = \max_{\|x\|_p=1} \|Ax\|_p$, $\forall p \in \mathbb{N} \cup \{0, \infty\}$. Then $\|A\|_\infty = \max_i \sum_j |A_{ij}|$, $\|A\|_1 = \max_j \sum_i |A_{ij}|$ and $\|A\|_2 = \sigma_{\max}(A)$, the maximum singular value. $\mathbf{1}$ is all ones vector with appropriate dimensions and \mathbf{I} is identity matrix with appropriate dimensions. $[n] = \{1, 2, \dots, n\}$, $\forall n \geq 1$. For a vector $x \in \mathbb{R}^n$, x_i ($i \in [n]$) is its i -th coordinate.

For the sake of proof we will assume that \mathcal{F} is class of vector functions of the form $D(x) \in \mathbb{R}^m$. In terms of the notation in the main material original $D(x, y)$ is $D(x)_y$ here. For a class \mathcal{F} of vector valued functions $D : \mathcal{X} \rightarrow \mathbb{R}^n$. Therefore we re-define the operation \circ between a matrix $T \in \mathbb{R}^{n \times n}$ and \mathcal{F} as,

$$T \circ \mathcal{F} = \{TD(\cdot) \mid f(\cdot) \in \mathcal{F}\}.$$

If $P_{X,Y}$ is probability distribution of $(X, Y) \in \mathcal{X} \times [m]$, then $P_{Y|X=x}$ is the conditional discrete distribution of Y given $X = x$, $p_X(x)$ is the marginal density of X , and

$$\bar{P}_{Y|X=x} = [P_{Y|X=x}(Y=1), P_{Y|X=x}(Y=1), \dots, P_{Y|X=x}(Y=m)]^T, \text{ and} \quad (18)$$

$$\bar{p}_X(x) = p_X(x)\bar{P}_{Y|X=x} \quad (19)$$

A.2 Supporting Lemmas

Lemma 1 (Characterization of neural network distance). $d_{\mathcal{F}, \phi}(P, Q) \geq 0$ for all P, Q . And if ϕ is a convex or concave function, then the Neural network distance is 0 when the distributions are same, i.e. $d_{\mathcal{F}, \phi}(P, P) = 0$.

Proof. For concave $\phi(\cdot)$ we define $\mu_\phi = \phi(1/2)$. Since, by definition $D = 1/2 \mathbf{1}$ is feasible solution to the optimization problem in (5), thus $d_{\mathcal{F}, \phi}(P, Q) \geq 0$.

$$\begin{aligned} d_{\mathcal{F}, \phi}(P, P) &= \sup_{D \in \mathcal{F}} \mathbb{E}_{(x,y) \sim P} [\phi(D(x)_y)] + \mathbb{E}_{(x,y) \sim P} [\phi(1 - D(x)_y)] - 2\phi(1/2) \\ &\leq \sup_{D \in \mathcal{F}} 2\phi\left(\mathbb{E}_{(x,y) \sim P} \left[\frac{1}{2}(D(x)_y + 1 - D(x)_y)\right]\right) - 2\phi(1/2) \\ &= \sup_{D \in \mathcal{F}} 2\phi(1/2) - 2\phi(1/2) = 0 \end{aligned}$$

The inequality in second line follows from Jensen's inequality for concave $\phi(\cdot)$.

For convex $\phi(\cdot)$ we define $\mu_\phi = \phi(0) + \phi(1)$. Since, by definition $D = 1$ is feasible solution to the optimization problem in (5), thus $d_{\mathcal{F}, \phi}(P, Q) \geq 0$.

$$\begin{aligned} d_{\mathcal{F}, \phi}(P, P) &= \sup_{D \in \mathcal{F}} \mathbb{E}_{(x,y) \sim P} [\phi(D(x)_y)] + \mathbb{E}_{(x,y) \sim P} [\phi(1 - D(x)_y)] - \phi(0) - \phi(1) \\ &= \sup_{D \in \mathcal{F}} \mathbb{E}_{(x,y) \sim P} [\phi(D(x)_y) + \phi(1 - D(x)_y)] - (\phi(0) + \phi(1)) \\ &\leq \sup_{D \in \mathcal{F}} \mathbb{E}_{(x,y) \sim P} [\phi(0) + \phi(1)] - (\phi(0) + \phi(1)) = 0 \end{aligned}$$

The last inequality follows from Jensen's inequality for convex $\phi(\cdot)$

□

This Lemma 1 ensures that all the multiplicative lower bounds and upper bounds in Theorem 3 and its corollaries implies recoverability.

Lemma 2. *If P is a distributions on $\mathcal{X} \times [m]$ and \tilde{P} is the distribution of sample (X, \tilde{Y}) of P when passed through the noisy-channel given by the confusion matrix $C \in \mathbb{R}^{m \times m}$ (as defined in Section 1). Then,*

$$\tilde{P}_{\tilde{Y}|X=x} = C^T \bar{P}_{Y|X=x}, \quad (20)$$

where $\bar{P}_{Y|X=x} = [P_{Y|X=x}(Y=1), P_{Y|X=x}(Y=1), \dots, P_{Y|X=x}(Y=m)]^T$.

Proof.

$$\begin{aligned} \tilde{P}_{\tilde{Y}|X=x}(\tilde{Y}=j) &= \sum_{i \in [m]} \mathbb{P}(\tilde{Y}=j | Y=i) P_{Y|X=x}(Y=j), \forall j \in [m] \\ \tilde{P}_{\tilde{Y}|X=x}(\tilde{Y}=j) &= \sum_{i \in [m]} C_{ij} P_{Y|X=x}(Y=j), \forall j \in [m] \\ \tilde{P}_{\tilde{Y}|X=x} &= C^T \bar{P}_{Y|X=x} \end{aligned}$$

□

B Proof of Theorem 1

We first prove the approximation bounds for total variation distance in Eq. (3), and then use it to prove similar bounds for the Jensen-Shannon divergence in Eq. (4). Recall that total variation distance between P and Q can be written in several ways:

$$\begin{aligned} d_{\text{TV}}(P, Q) &= \max_{S_1, \dots, S_m} \sum_{y \in [m]} P(S_y, y) - Q(S_y, y) \\ &= \max_{S_1, \dots, S_m} \sum_{y \in [m]} |P(S_y, y) - Q(S_y, y)| \\ &= \max_{S_1, \dots, S_m} \|P(\{S_y\}_{y \in [m]}, \cdot) - Q(\{S_y\}_{y \in [m]}, \cdot)\|_1, \end{aligned}$$

where we used the notation of a row-vector $P(\{S_y\}_{y \in [m]}, \cdot) = [P(S_1, 1), \dots, P(S_m, m)]$. The lower bound on $d_{\text{TV}}(\tilde{P}, \tilde{Q})$ follows that

$$\begin{aligned} d_{\text{TV}}(P, Q) &= \max_{S_1, \dots, S_m \subseteq \mathcal{X}} \sum_{y \in [m]} \{P(S_y, y) - Q(S_y, y)\} \\ &= \max_{S_1, \dots, S_m \subseteq \mathcal{X}} \langle \mathbf{1}, P(\{S_y\}_{y \in [m]}, \cdot) - Q(\{S_y\}_{y \in [m]}, \cdot) \rangle \\ &\stackrel{(a)}{=} \max_{S_1, \dots, S_m \subseteq \mathcal{X}} \langle \mathbf{1}, (\tilde{P}(\{S_y\}_{y \in [m]}, \cdot) - \tilde{Q}(\{S_y\}_{y \in [m]}, \cdot)) C^{-1} \rangle \\ &\stackrel{(b)}{\leq} \|C^{-T}\|_1 \max_{S_1, \dots, S_m \subseteq \mathcal{X}} \|\tilde{P}(\{S_y\}_{y \in [m]}, \cdot) - \tilde{Q}(\{S_y\}_{y \in [m]}, \cdot)\|_1 \\ &\stackrel{(c)}{=} \|C^{-1}\|_\infty d_{\text{TV}}(\tilde{P}, \tilde{Q}), \end{aligned}$$

where (a) follows from the fact that $\tilde{P}(\{S_y\}_{y \in [m]}, \cdot) = P(\{S_y\}_{y \in [m]}, \cdot) C$, (b) follows from the fact that $\mathbf{1}^T A x \leq \|A x\|_1 \leq \|A\|_1 \|x\|_1$, and (c) follows from $\|A\|_1 = \|A^T\|_\infty$. The upper bound follows from similar

arguments:

$$\begin{aligned} d_{\text{TV}}(\tilde{P}, \tilde{Q}) &\leq \|C^T\|_1 \max_{S_1, \dots, S_m \subseteq \mathcal{X}} \|P(\{S_y\}_{y \in [m]}, \cdot) - Q(\{S_y\}_{y \in [m]}, \cdot)\|_1 \\ &= d_{\text{TV}}(P, Q) \end{aligned}$$

where last equality uses the fact that $\|C^T\|_1 = 1$ for all row-stochastic matrices C .

To prove the approximation bounds for Jensen-Shannon divergence, we use the following lemma that bounds the JS divergence by the TV distance.

Lemma 3. $\frac{1}{2}d_{\text{TV}}(P, Q)^2 \leq d_{\text{JS}}(P \parallel Q) \leq 2d_{\text{TV}}(P, Q)$.

A proof is provided in Section B.1. The following series of inequalities follow from this lemma.

$$\begin{aligned} \frac{1}{2}d_{\text{TV}}(\tilde{P}, \tilde{Q})^2 &\stackrel{(a)}{\leq} d_{\text{JS}}(\tilde{P} \parallel \tilde{Q}) \stackrel{(a)}{\leq} 2d_{\text{TV}}(\tilde{P}, \tilde{Q}) \\ \frac{\|C^{-1}\|_\infty^{-2}}{2}d_{\text{TV}}(P, Q)^2 &\stackrel{(b)}{\leq} d_{\text{JS}}(\tilde{P} \parallel \tilde{Q}) \stackrel{(b)}{\leq} 2d_{\text{TV}}(P, Q) \\ \frac{\|C^{-1}\|_\infty^{-2}}{8}d_{\text{JS}}(P \parallel Q)^2 &\stackrel{(a)}{\leq} d_{\text{JS}}(\tilde{P} \parallel \tilde{Q}) \stackrel{(a)}{\leq} \sqrt{8d_{\text{JS}}(P \parallel Q)} \end{aligned}$$

where (a) uses Lemma 3, and (b) uses equation (3).

B.1 Proof of Lemma 3

$$\begin{aligned} d_{\text{KL}}\left(P \parallel \frac{P+Q}{2}\right) &= \mathbb{E}_{X \sim P} \left[\log \frac{2P(X)}{P(X) + Q(X)} \right] \\ &\stackrel{(a)}{\leq} \mathbb{E}_{X \sim P} \left[\frac{2P(X) - (P(X) + Q(X))}{P(X) + Q(X)} \right] \\ &\leq \sup_X \frac{2P(X)}{P(X) + Q(X)} \cdot \mathbb{E}_{X \sim P} \left[\frac{|2P(X) - (P(X) + Q(X))|}{2P(X)} \right] \\ &\leq 2 \cdot 2d_{\text{TV}}\left(P, \frac{P+Q}{2}\right) \\ &\leq 2d_{\text{TV}}(P, Q), \end{aligned} \tag{21}$$

where (a) uses $\log x \leq x - 1$.

$$\begin{aligned} d_{\text{JS}}(P \parallel Q) &= \frac{1}{2}d_{\text{KL}}\left(P \parallel \frac{P+Q}{2}\right) + \frac{1}{2}d_{\text{KL}}\left(Q \parallel \frac{P+Q}{2}\right) \\ &\stackrel{(b)}{\geq} d_{\text{TV}}\left(P, \frac{P+Q}{2}\right)^2 + d_{\text{TV}}\left(Q, \frac{P+Q}{2}\right)^2 \\ &= \frac{1}{2}d_{\text{TV}}(P, Q)^2 \end{aligned}$$

where (a) uses equation (21), and (b) uses Pinsker's inequality $0.5d_{\text{KL}}(P \parallel Q) \leq d_{\text{TV}}(P, Q)^2$

C Examples satisfying Assumption 1

Several classes of functions that are used in practice and studied in theory indeed satisfy our Assumption 1. For example, consider the set of 1-Lipschitz continuous and bounded functions $\mathcal{F} = \{f : \mathbb{R}^d \times [m] \rightarrow \mathbb{R} \mid 0 \leq$

$f(x, y) \leq 1$ for all x and y , and $|f(x_1, y_1) - f(x_2, y_2)| \leq \|x_1 - x_2\| + |y_1 - y_2|$ for all x_1, x_2, y_1 , and y_2 , which was studied in [3] in the context of generalization bounds for the neural network distance. It follows that this \mathcal{F} satisfies Assumption 1, with $c = 1/2$ and $\mathcal{F} - 1/2 \in \mathcal{F}_1$. This is a special case of some examples of classes of functions satisfying the assumption, that we provide in the following Remark. A proof is provided in Appendix F.

Remark 3. *The following classes of discriminators satisfy the inclusion condition in Assumption 1:*

1. *Class of all bounded functions $D : \mathcal{X} \times [m] \rightarrow [c_1, c_2]$ for any $c_1 \leq c_2 \in \mathbb{R}$.*
2. *Class of all bounded functions $D : \mathcal{X} \times [m] \rightarrow [c_1, c_2]$, which are L -Lipschitz in x for any $c_1 \leq c_2 \in \mathbb{R}$ and $L \geq 0$.*
3. *Class of all bounded functions $D : \mathcal{X} \times [m] \rightarrow [c_1, c_2]$, which are L -Lipschitz in x and y for any $c_1 \leq c_2 \in \mathbb{R}$ and $L \geq (c_2 - c_1)$.*

D Proof of Remark 1: the tightness of Theorem 2

Let $\mathcal{X} = \{x_1, x_2\}$ and $\mathcal{F} = \{f \mid f(x, y) \in [-1, 1]\}$. From Remark 3, we know that \mathcal{F} satisfies Assumption 1. Then it is easy to check that $d_{\mathcal{F}}(P, Q) = \|P - Q\|_1 + \|P - Q\|_1$, where we used the notation $P(\{x\}, \cdot) = [P(\{x\}, 1), \dots, P(\{x\}, m)]$.

1. **Lower bound:** It is easy to show that there exists $P_{X,Y}$ and $Q_{X,Y}$ such that $(P - Q)(\{x_1\}, \cdot) = \epsilon \mathbf{1}$ and $(P - Q)(\{x_2\}, \cdot) = -\epsilon \mathbf{1}$ for any $\epsilon \in [0, 1/m]$. Thus,

$$d_{\mathcal{F}}(P, Q) = \|\epsilon \mathbf{1}\|_1 + \|-\epsilon \mathbf{1}\|_1 = 2m\epsilon. \quad (22)$$

Then we can show that,

$$(\tilde{P} - \tilde{Q})(\{x\}, \cdot) = C^T(P - Q)(\{x\}, \cdot) = \pm \epsilon C^T \mathbf{1} \quad (23)$$

Thus,

$$d_{\mathcal{F}}(\tilde{P}, \tilde{Q}) = 2\|\pm \epsilon C^T \mathbf{1}\|_1 = 2\epsilon \mathbf{1}^T C^T \mathbf{1} = 2\epsilon \mathbf{1}^T \mathbf{1} = 2m\epsilon, \quad (24)$$

where the penultimate equality follow from $C\mathbf{1} = \mathbf{1}$, since C is row-stochastic.

2. **Upper bound:** We can again show that there exists $P_{X,Y}$ and $Q_{X,Y}$ such that $(P - Q)(\{x_1\}, \cdot) = \epsilon C^{-T} v$ and $(P - Q)(\{x_2\}, \cdot) = -\epsilon C^{-T} v$, where $v \in \arg \max_{v_i \in \pm 1} \|C^{-T} v\|_1$, for sufficiently small ϵ . Thus,

$$d_{\mathcal{F}}(P, Q) = 2\|\pm \epsilon C^{-T} v\|_1 = 2\epsilon \|C^{-T}\|_1 \|v\|_1 = 2\epsilon \|C^{-1}\|_{\infty} \|v\|_1. \quad (25)$$

Using similar steps as the above lower-bound case, we can show that,

$$d_{\mathcal{F}}(\tilde{P}, \tilde{Q}) = 2\|\pm \epsilon C^T C^{-T} v\|_1 = 2\epsilon \|v\|_1. \quad (26)$$

E Proof of Theorem 2

We start with the following two key lemmas.

Lemma 4. *For any sample $(X, Y) \sim P$ (or Q), let \tilde{P} (or \tilde{Q}) denote the sample whose label Y is corrupted by a noise defined by a confusion matrix C , where $C_{y\tilde{y}}$ is the probability the a label y is corrupted as a label \tilde{y} . Then, for any P, Q , and any class of discriminators \mathcal{F} ,*

$$d_{\mathcal{F}}(\tilde{P}, \tilde{Q}) = d_{C \circ \mathcal{F}}(P, Q). \quad (27)$$

Lemma 5. If a class of discriminators \mathcal{F} satisfies Assumption 1 with a constant shift c , then for all row-stochastic non-negative matrix C ,

$$\|C^{-1}\|_{\infty}^{-1} \mathbf{I} \circ (\mathcal{F} - c) \subseteq C \circ (\mathcal{F} - c) \subseteq (\mathcal{F} - c). \quad (28)$$

From the ordering of sets of functions in Lemma 5, it follows that

$$d_{C \circ \mathcal{F}}(P, Q) \geq d_{\|C^{-1}\|_{\infty}^{-1} \mathbf{I} \circ \mathcal{F}}(P, Q) = \|C^{-1}\|_{\infty}^{-1} d_{\mathcal{F}}(P, Q) \quad (29)$$

where the last equality follows from the fact that $D \in \mathcal{F}$ if and only if $\alpha D \in \alpha \mathbf{I} \circ \mathcal{F}$. Note that we ignored the shift c , as the definition of the neural network distance is invariant to any constant shift c , and we can cancel any given shift c of a set \mathcal{F} as we see fit. Next, it follows immediately from Lemma 5 that

$$d_{C \circ \mathcal{F}}(P, Q) \leq d_{\mathcal{F}}(P, Q). \quad (30)$$

This finishes the proof of the theorem.

E.1 Proof of Lemma 4

For any function $D : \mathcal{X} \times [m] \rightarrow \mathbb{R}$ and a distribution P over $\mathcal{X} \times [m]$, we denote the expectation by $\langle D, P \rangle = \mathbb{E}_{(X, Y) \sim P}[D(X, Y)]$. Further, we let $\tilde{P}(S, \tilde{y}) = \sum_y P(S, y)C_{y\tilde{y}} = PC(S, \tilde{y})$ denote the distribution of the corrupted sample, by noise with confusion matrix C . Note that we intentionally overloaded the matrix multiplication notation PC . We also treat D as a (infinite-dimensional) matrix, and let $DC^T(x, y) = \sum_{\tilde{y}} D(x, \tilde{y})C_{y\tilde{y}}$. It follows that,

$$\begin{aligned} d_{\mathcal{F}}(\tilde{P}, \tilde{Q}) &\triangleq \sup_{D \in \mathcal{F}} \mathbb{E}_{\tilde{P}}[D(X, Y)] - \mathbb{E}_{\tilde{Q}}[D(X, Y)] \\ &= \sup_{D \in \mathcal{F}} \langle D, \tilde{P} - \tilde{Q} \rangle \\ &= \sup_{D \in \mathcal{F}} \langle D, (P - Q)C \rangle \\ &= \sup_{D \in \mathcal{F}} \langle DC^T, (P - Q) \rangle \\ &= \sup_{\tilde{D} \in C \circ \mathcal{F}} \langle \tilde{D}, (P - Q) \rangle, \end{aligned}$$

where the last equality follows from the definition of the \circ operation in Eq. (6). This proves the desired claim.

E.2 Proof of Lemma 5

We will prove the desired claim for \mathcal{F}_1 and \mathcal{F}_2 separately. As the set orderings are preserved under addition of sets, this proves the desired claim.

First we will prove the Lemma when condition $T \circ \mathcal{F} \subseteq \mathcal{F}$ holds. We use the notations from Appendix E.1. We want to prove,

$$\begin{aligned} &\|C^{-1}\|_{\infty}^{-1} \mathbf{I} \circ \mathcal{F} \subseteq C \circ \mathcal{F} \\ \iff &\forall D \in \mathcal{F}, \exists D' \in \mathcal{F} \text{ such that } \|C^{-1}\|_{\infty}^{-1} D(x, y) = D' C^T(x, y), \quad \forall x \in \mathcal{X}, \forall y \in [m] \\ \iff &\forall D \in \mathcal{F}, \exists D' \in \mathcal{F} \text{ such that } \|C^{-1}\|_{\infty}^{-1} DC^{-T}(x, y) = D'(x, y), \quad \forall x \in \mathcal{X}, \forall y \in [m] \\ \iff &\|C^{-1}\|_{\infty}^{-1} C^{-1} \circ \mathcal{F} \subseteq \mathcal{F}. \end{aligned}$$

The last statement is true by the the Assumption 1 because $\| (C^{-1}/\|C^{-1}\|_{\infty}) \|_{\infty} = 1$. The second covering $C \circ \mathcal{F} \subseteq \mathcal{F}$ is also true by Assumption 1 because $\|C\|_{\infty} = 1$ since C is row-stochastic matrix with rows summing to 1.

Now we will prove the case when condition $\mathcal{F} = \{\alpha f(x) \mid f(x)_y = g(x) \in \mathbb{R}, g \in \mathcal{F}_x, \alpha \in [0, 1]\}$ holds. $C \circ \mathcal{F} \subseteq \mathcal{F}$ holds true because $\mathbf{1}$ is an eigenvector of C with eigenvalue 1. Similarly to the previous condition, we need to prove that $C^{-1}/\|C^{-1}\|_\infty \circ \mathcal{F} \subseteq \mathcal{F}$, but since $\mathbf{1}$ is an eigenvector of C^{-1} with eigenvalue $1/\|C^{-1}\|_\infty \leq 1$, the again holds true.

F Proof of Remarks 3 and 2

F.1 Class of all bounded functions (Total Variation)

Let $\mathcal{F}([c_1, c_2])$ be class of all functions with range inside $[c_1, c_2]^m$. Proof follows from the Appendix F.2 by taking $\lim_{L \rightarrow \infty}$.

F.2 Class of all bounded and Lipschitz functions in x

Let $\mathcal{F}(L, [c_1, c_2])$ be class of all vector valued L -Lipschitz functions in x with range inside $[c_1, c_2]^m$. That is,

$$\|D(x_1) - D(x_2)\|_\infty \leq L \|x_1 - x_2\|_2 \text{ and } D(x) \in [c_1, c_2] \quad \forall x, x_1, x_2 \in \mathcal{X}, y \in [m] \quad (31)$$

Lemma 6. $d_{\mathcal{F}(L, [c_1, c_2])}(P, Q) = \frac{(c_2 - c_1)}{2} d_{\mathcal{F}(2L/(c_2 - c_1), [-1, 1])}(P, Q)$

Proof. There exists a bijection $f : \mathcal{F}(L, [c_1, c_2]) \rightarrow \mathcal{F}(2L/(c_2 - c_1), [-1, 1])$, such that $f(D) = \frac{2D - (c_1 + c_2)}{c_2 - c_1}$. This is true since f is invertible, $f(D) \in [-1, 1]$, and f is $2L/(c_2 - c_1)$ -Lipschitz.

$$\begin{aligned} d_{\mathcal{F}(L, [c_1, c_2])}(P, Q) &= \sup_{D \in \mathcal{F}(L, [c_1, c_2])} \mathbb{E}_{(x,y) \sim P} [D(x, y)] - \mathbb{E}_{(x,y) \sim Q} [D(x, y)] \\ &= \frac{(c_2 - c_1)}{2} \sup_{D \in \mathcal{F}(2L/(c_2 - c_1), [-1, 1])} \mathbb{E}_{(x,y) \sim P} [f(D)(x, y)] - \mathbb{E}_{(x,y) \sim Q} [f(D)(x, y)] \\ &= \frac{(c_2 - c_1)}{2} d_{\mathcal{F}(2L/(c_2 - c_1), [-1, 1])}(P, Q) \end{aligned} \quad (32)$$

□

By Lemma 6 any $[c_1, c_2]$ is similar to $[-1, 1]$ up to a scaling, thus we only prove for $[-1, 1]$. Now we will show that the inclusion condition (Assumption 1) hold for this class of functions.

Lemma 7. $T \circ \mathcal{F}(L, [-1, 1]) \subseteq \mathcal{F}(L, [-1, 1])$, $\forall \|T\|_\infty = 1$

Proof. We want to show that, $\forall D' \in T \circ \mathcal{F}(L, [-1, 1])$, we also have $D' \in \mathcal{F}(L, [-1, 1])$. In other words, $\forall D \in \mathcal{F}(L, [-1, 1])$, $TD \in \mathcal{F}(L, [-1, 1])$. First the we show that range of $D \in T \circ \mathcal{F}(L, [-1, 1])$ is $[-1, 1]$, ie.,

$$\|TD(x)\|_\infty \leq \|T\|_\infty \|D(x)\|_\infty \leq 1 \cdot 1 \leq 1. \quad (33)$$

In a similar way we prove the Lipschitz property.

$$\|TD(x_1) - TD(x_2)\|_\infty \leq \|T\|_\infty \|D(x_1) - D(x_2)\|_\infty \leq 1 \cdot L \|x_1 - x_2\|_2 \quad (34)$$

□

Finally, we can use Theorem 2 to get the desired result.

F.3 Class of all bounded and Lipschitz functions in x and y

As $|y_1 - y_2| \geq 1$ for all $y_1 \neq y_2$, L -Lipschitz functions with $L \geq c_2 - c_1$ only imposes conditions on pairs of data with the same values of y . Hence, this boils down to the previous case studied in Appendix F.2.

F.4 Class of projection discriminators

The function class is $\mathcal{F} = \{f_1 + f_2 \mid f_1 \in \mathcal{F}_1^{(\theta)}, f_2 \in \mathcal{F}_2^{(\theta)}, \theta \in \mathbb{R}^{d_\theta}\}$, where

$$\mathcal{F}_1^{(\theta)} = \{\text{vec}(y)^T V \psi(x; \theta) \mid V \in \mathcal{V}_1\}, \text{ and,} \quad (35)$$

$$\mathcal{F}_2^{(\theta)} = \{v^T \psi'(x; \theta) \mid v \in \mathcal{V}_2\}, \text{ where,} \quad (36)$$

$$\mathcal{V}_1 = \{V \in \mathbb{R}^{m \times d_V} \mid \max_i |V_{ij}| \leq 1 \text{ for all } j \in [d_V]\}, \text{ and} \quad (37)$$

$$\mathcal{V}_2 = \{v \in \mathbb{R}^{d_v} \mid \|v\| \leq 1\}. \quad (38)$$

We will show that both $\mathcal{F}_1^{(\theta)}$ and $\mathcal{F}_2^{(\theta)}$ satisfy Assumption 1. For any $A \in \mathbb{R}^{m \times m}$, we can write $A \circ \mathcal{F}_1^{(\theta)}$ as

$$A \circ \mathcal{F}_1^{(\theta)} = \{\text{vec}(y)^T AV \psi(x; \theta) \mid V \in \mathcal{V}_1\}. \quad (39)$$

If $\|A\|_\infty = 1$, then, $\max_{i \in [m]} |(AV)_{ij}| = \|(AV)_{\cdot,j}\|_\infty = \|A(V_{\cdot,j})\|_\infty \leq \|A\|_\infty \|V_{\cdot,j}\|_\infty = 1 \cdot \max_{i \in [m]} |V_{ij}| \leq 1$, which implies than $AV \in \mathcal{V}_1$. Thus $\mathcal{F}_1^{(\theta)}$ satisfies inclusion condition, $A \circ \mathcal{F}_1^{(\theta)} \subseteq \mathcal{F}_1^{(\theta)}$. Since

$$\mathcal{V}_2 = \{v \in \mathbb{R}^{d_v} \mid \|v\| \leq 1\} = \{\alpha v \mid v \in \mathbb{R}^{d_v}, \|v\| = 1, \alpha \in [0, 1]\} \quad (40)$$

we can re-write $\mathcal{F}_2^{(\theta)}$ as,

$$\mathcal{F}_2^{(\theta)} = \left\{ \alpha f(x, y) \mid f(x, y) = f(x), f(x) \in \mathcal{G}^{(\theta, x)} = \{v^T \psi'(x; \theta) \mid \|v\| = 1\}, \alpha \in [0, 1] \right\}. \quad (41)$$

Thus $\mathcal{F}_2^{(\theta)}$ satisfies the label invariance condition. Finally, since Assumption 1 holds true for $\mathcal{F}_1^{(\theta)}$ and $\mathcal{F}_2^{(\theta)}$, it also holds for \mathcal{F} .

G Proof of Theorem 3

Let $\mathcal{F} = \{D \mid D(x) \in [-1, 1]^m\}$. We show that,

$$\begin{aligned} \mathcal{F}_3 &= \left\{ D \in \mathcal{F} \mid |D(x)^T C^T (\bar{p}(x) - \bar{q}(x))| \leq \epsilon \forall x \in \mathcal{X} \right\}. \\ \mathcal{F}_4 &= \left\{ D \in \mathcal{F} \mid |D(x)^T (\bar{p}(x) - \bar{q}(x))| \leq \epsilon \forall x \in \mathcal{X} \right\} \end{aligned}$$

Then,

$$\begin{aligned}
d_{\mathcal{F}_3}(\tilde{P}, \tilde{Q}) &= \sup_{D \in \mathcal{F}} \mathbb{E}_{(x,y) \sim \tilde{P}} [D(x)_y] - \mathbb{E}_{(x,y) \sim \tilde{Q}} [D(x)_y] \\
&= \sup_{D \in \mathcal{F}} \mathbb{E}_{(x,y) \sim P} [(CD(x))_y] - \mathbb{E}_{(x,y) \sim Q} [(CD(x))_y] \\
&= \sup_{D \in \mathcal{F}} \int_{\mathcal{X}} D(x)^T C^T (p(x) P_{Y|X=x}(y)) - q(x) Q_{Y|X=x}(y) \\
&\leq \sup_{D \in \mathcal{F}} \int_{\mathcal{X}} \epsilon = O(\epsilon) \\
d_{\mathcal{F}_3}(P, Q) &= \sup_{D \in \mathcal{F}} \mathbb{E}_{(x,y) \sim P} [D(x)_y] - \mathbb{E}_{(x,y) \sim Q} [D(x)_y] \\
&= \sup_{D \in \mathcal{F}} \int_{\mathcal{X}} D(x)^T (p(x) \bar{P}_{Y|X=x} - q(x) \bar{Q}_{Y|X=x}) \\
&\geq \sup_{D \in \mathcal{F}} \int_{\mathcal{X}_S} D(x)^T (p(x) \bar{P}_{Y|X=x} - q(x) \bar{Q}_{Y|X=x}) \\
&\stackrel{(a)}{\geq} \sup_{\substack{D \in \mathcal{F} \\ D(x) \perp v_x}} \int_{\mathcal{X}_S} D(x)^T u_x \\
&= \sup_{D \in \mathcal{F}} \int_{\mathcal{X}_S} D(x)^T (u_x - (u_x^T \hat{v}_x) \hat{v}_x) \\
&= \sup_{D \in \mathcal{F}} \int_{\mathcal{X}_S} \|u_x - (u_x^T \hat{v}_x) \hat{v}_x\|_1,
\end{aligned}$$

where in (a) we put $p(x)P_{Y|X=x}(y) - q(x)Q_{Y|X=x}(y) = u_x$ and $C^T u_x = v_x$. Since u_x is not an eigenvector of C , $u_x \not\perp v_x$ and therefore the integrand is positive. Finally using the assumption that $P_X(\mathcal{X}_S) + Q_X(\mathcal{X}) > 0$ we get that LHS is positive number. Now by taking ϵ much smaller than the LHS we get the desired result. Other case also follows similarly.

H Proof of Theorem 4

Proposition 1. *There exists a class \mathcal{F} of parametric vector valued functions which satisfy the Lipschitzness in parameters property (14), such that $\mathcal{F} - 1/2\mathbb{1}$ satisfies the inclusion condition (Assumption 1).*

Proof. For the proof we show that there exists a class of discriminators which satisfy the inclusion condition of Assumption 1 and in particular we have the following example. Let \mathcal{F}' be a class of vector functions parameterized by the $u' \in \mathcal{U}'$ which is L' -Lipschitz in the parameters and whose element functions satisfy $\|f_{u'}(x)\|_\infty \leq 1/2$. We define a new class of vector functions

$$\bar{\mathcal{F}} \triangleq \{T' f_{u'}(\cdot) + 1/2 \mathbb{1} \mid \forall f(\cdot) \in \mathcal{F}', \|T'\|_\infty \leq 1\}, \quad (42)$$

parameterized by $u = (u', T') \in \mathcal{U}' \times \{T' \mid \|T'\|_\infty \leq 1\}$. Then,

$$\begin{aligned}
\|T'_1 D_{u'_1}(x, \cdot) - T'_2 D_{u'_2}(x, \cdot)\|_\infty &\stackrel{(a)}{\leq} \|T'_1 D_{u'_1}(x, \cdot) - T'_2 D_{u'_1}(x, \cdot)\|_\infty + \|T'_2 D_{u'_1}(x, \cdot) - T'_2 D_{u'_2}(x, \cdot)\|_\infty \\
&\stackrel{(b)}{\leq} \|T'_1 D_{u'_1}(x, \cdot) - T'_2 D_{u'_1}(x, \cdot)\|_2 + \|T'_2\|_\infty \|D_{u'_1}(x, \cdot) - D_{u'_2}(x, \cdot)\|_\infty \\
&\stackrel{(c)}{\leq} \|T'_1 - T'_2\|_2 \|D_{u'_1}(x, \cdot)\|_2 + \|T'_2\|_\infty L' \|u'_1 - u'_2\|_2 \\
&\stackrel{(d)}{\leq} \|T'_1 - T'_2\|_2 \sqrt{m} + L' \|u'_1 - u'_2\|_2 \\
&\leq (\sqrt{m} + L') (\|T'_1 - T'_2\|_2 + \|u'_1 - u'_2\|_2) \\
&\stackrel{(e)}{\leq} \sqrt{2}(\sqrt{m} + L') \sqrt{\|T'_1 - T'_2\|_2^2 + \|u'_1 - u'_2\|_2^2}
\end{aligned} \tag{43}$$

where (a) uses triangle inequality, (b) and (c) uses $\|x\|_\infty \leq \|x\|_2$ and $\|Ax\|_p \leq \|A\|_p \|x\|_p$ (see Section 1), (c) is true since $\bar{\mathcal{F}}'$ is L' -Lipschitz in u' , (d) uses $\|D_{u'}(x, \cdot)\|_\infty \leq 1/2$ and $\|T'_2\|_\infty \leq 1$, and (e) uses $x + y \leq \sqrt{2(x^2 + y^2)}$.

Next we show that \mathcal{F} lies in the range $[0, 1]^m$ as follows.

$$\|T' D_{u'}(x, \cdot)\|_\infty \leq \|T'\|_\infty \|D_{u'}(x, \cdot)\|_\infty \stackrel{(b)}{\leq} 1 \cdot 1/2 \tag{44}$$

We can prove inclusion condition in Assumption 1 by the fact that $\|TT'\|_\infty \leq \|T\|_\infty \|T'\|_\infty \leq 1 \cdot 1$ and hence TT' is valid choice for T . \square

Next we present a straightforward corollary of Theorem 2.

Theorem 5. Let \mathcal{F} be a parametric class of vector valued functions parameterized by $u \in \mathcal{U} \subseteq \mathbb{R}^p$ such that $f_u : \mathcal{X} \rightarrow [0, 1]^m$, $\forall f_u \in \mathcal{F}$. Further, if \mathcal{F} is L -Lipschitz in the parameter u , as defined in equation (14), and if \mathcal{F} satisfies Assumption 1, then,

$$d_{\mathcal{F}}(\tilde{P}, \tilde{Q}) \leq d_{\mathcal{F}}(P, Q) \leq \|C^{-1}\|_\infty d_{\mathcal{F}}(\tilde{P}, \tilde{Q}) \tag{45}$$

Proof. Proof directly follows from Theorem 2, since $T \circ \mathcal{F}$ preserves Lipschitzness in u , when $\|T\|_\infty = 1$. \square

Corollary 1 (of [3], Theorem 3.1.). Assume the same class \mathcal{F} as in Theorem 5. Let \tilde{P}, \tilde{Q} be two distributions on X, \tilde{Y} and be \tilde{P}_n, \tilde{Q}_n be empirical versions of them with at least n samples each. Then there is universal constant c such that when $n \geq \frac{c p \log(pL/\epsilon)}{\epsilon^2}$, we have with probability at least $1 - \exp(-p)$ over the randomness of \tilde{P}_n, \tilde{Q}_n ,

$$\left| d_{\mathcal{F}}(\tilde{P}_n, \tilde{Q}_n) - d_{\mathcal{F}}(\tilde{P}, \tilde{Q}) \right| \leq \epsilon \tag{46}$$

Proof. Proof is directly follow from [3][Theorem 3.1]. \square

$$\begin{aligned}
d_{\mathcal{F}}(\tilde{P}, \tilde{Q}) &\stackrel{(a)}{\leq} d_{\mathcal{F}}(P, Q) \stackrel{(a)}{\leq} \|C^{-1}\|_\infty d_{\mathcal{F}}(\tilde{P}, \tilde{Q}) \\
d_{\mathcal{F}}(\tilde{P}_n, \tilde{Q}_n) - \epsilon &\stackrel{(a)}{\leq} d_{\mathcal{F}}(P, Q) \stackrel{(a)}{\leq} \|C^{-1}\|_\infty (d_{\mathcal{F}}(\tilde{P}_n, \tilde{Q}_n) + \epsilon)
\end{aligned}$$

where (a) is true by Theorem 5 and (b) is true from the Corollary 1.

I Implementation details

Hyperparameters and architectures for MNIST: Biased GAN uses the standard conditional DCGAN architecture [37] implementation². RCGAN, RCGAN-U, and unbiased GAN use the same DCGAN architecture [37] with hinge loss, $\phi(a) = \max(0, 1 - 2a)$, and conditional projection discriminator [32], as suggested by our theoretical analysis. Additionally, we also present RCGAN+y architecture, which has the same architecture as RCGAN but the input to the first layer of its discriminator is concatenated with a one-hot representation of the label.

We use $\lambda = 0$ and $\lambda = 1$ for RCGAN and RCGAN-U respectively, and a linear classifier for the permutation regularizer. For RCGAN-U, the learning rate of the confusion matrix is 10 times as that of the discriminator and the generator.

RCGAN+y training: RCGAN+y architecture has the same architecture as RCGAN but the input to the first layer of its discriminator is concatenated with a one-hot representation of the label. We observed that RCGAN+y is harder to train especially at low noise regimes of $\alpha \geq 0.4$. To combat this we add additional artificial noise, parameterized by $\tilde{\alpha}$, so that the effective noise parameter is $\bar{\alpha} = \tilde{\alpha}(\alpha - \frac{(1-\alpha)}{9}) + \frac{(1-\alpha)}{9}$. We schedule $\tilde{\alpha}$ during the training so that from epoch 0 to 30, the effective noise $\bar{\alpha} = 0.3$. When the original noise parameter α value is 0.9, from epoch 30 to 80, we linearly increase $\tilde{\alpha}$ so that the effective noise parameter linearly decrease from 0.3 to α , and from epoch 80 to 100 we keep the artificial noise parameter $\tilde{\alpha}$ to 1, so that effective noise parameter $\bar{\alpha} = \alpha$. For original noise parameter α value less than 0.9, starting from epoch 30 we increase $\tilde{\alpha}$ in the same rate as in the case of $\alpha = 0.9$ and once it reaches 1 keep it constant till the end of training. This stabilizes the training of RCGAN+y.

We suspect that the reason why RCGAN+y works better than RCGAN is that RCGAN+y optimizes over a larger class of functions, which might be necessary when learning a conditional distribution with large noise. Thus, as the noise increases it becomes more challenging for the projection discriminator to differentiate between \tilde{P} and \tilde{Q} , since it is much simpler function of y with y appearing only in the final layer. However, in RCGAN+y since we concatenate y to the input of the first layer, RCGAN+y discriminator may be able to better differentiate between \tilde{P} and \tilde{Q} .

Hyperparameters and architectures for CIFAR-10: We use ResNet based GAN used in [15] with spectral normalization [31] and conditional projection discriminator [32]³. We note that the spectral normalization work [31] reports higher inception score than what we achieved on the noiseless setting, possibly due to limited hyper-parameter tuning. For all the four approaches we use the same hyper-parameters.

We use $\lambda = 0$ and $\lambda = 1$ for RCGAN and RCGAN-U respectively, and a linear classifier for the permutation regularizer. For RCGAN-U, the learning rate of the confusion matrix is same as that of the discriminator and the generator.

RCGAN-U CIFAR-10 initialization: For CIFAR-10 dataset, we observed that even with the permutation regularizer, the learned confusion matrix in RCGAN-U was a permuted version of the true C , possibly because a linear classifier might be too simple to classify CIFAR images. To combat this, we initialized the confusion matrix M to be diagonally dominant. We initialized the confusion matrix to be learned M so that diagonal entries are 0.2 and off-diagonal entries are $(1 - 0.2)/9$. In our experiments, this ensured that the approximately true confusion matrix C was learned by M in RCGAN-U. We believe that better CIFAR-10 classifier for permutation regularizers can achieve the same effect as this initialization.

J Additional experimental information

In this section, we provide tables with the numerical values of the data points in the Figures 2 and 3.

²<https://github.com/carpedm20/DCGAN-tensorflow>

³https://github.com/watsonyanghx/GAN_Lib_Tensorflow

Noise ($1 - \alpha$)	RCGAN+y	RCGAN	RCGAN-U	unbiased GAN	biased GAN
0.875	0.905	0.11	0.215	0.1	0.119
0.85	0.984	0.211	0.235	0.1	0.138
0.8	0.987	0.44	0.489	0.1	0.192
0.7	0.985	0.978	0.992	0.1	0.288
0.6	0.976	0.983	0.991	0.2	0.375
0.5	0.976	0.991	0.986	0.869	0.475
0.4	0.984	0.994	0.99	0.997	0.57
0.3	0.983	0.994	0.987	0.991	0.681
0.2	0.99	0.994	0.995	0.999	0.765
0.1	0.99	0.994	0.995	0.998	0.873
0.0	0.995	0.995	0.994	0.994	0.994

Table 2: Numerical values for the datapoints in Figure 2 (left panel). Noisy MNIST dataset: Generated label accuracy of RCGAN, RCGAN-U, RCGAN+y, unbiased GAN and biased GAN.

Noise ($1 - \alpha$)	RCGAN+y	RCGAN	RCGAN-U	unbiased GAN	biased GAN
0.875	0.156	0.885	0.86	0.898	0.872
0.85	0.102	0.774	0.77	0.894	0.854
0.8	0.088	0.638	0.69	0.9	0.634
0.7	0.11	0.096	0.098	0.768	0.55
0.6	0.088	0.1	0.058	0.902	0.322
0.5	0.07	0.106	0.094	0.472	0.274
0.4	0.072	0.098	0.08	0.158	0.164
0.3	0.096	0.088	0.084	0.098	0.142
0.2	0.076	0.086	0.086	0.07	0.138
0.1	0.112	0.068	0.096	0.088	0.104
0.0	0.069	0.069	0.069	0.069	0.069

Table 3: Numerical values for the datapoints in Figure 2 (right panel). Noisy MNIST dataset: Label recovery error of RCGAN, RCGAN-U, RCGAN+y, unbiased GAN and biased GAN.

Noise ($1 - \alpha$)	RCGAN	RCGAN-U	unbiased GAN	biased GAN
0.8	0.111	0.126	0.110	0.117
0.6	0.443	0.263	0.1	0.148
0.4	0.700	0.71	0.4	0.340
0.2	0.724	0.815	0.6	0.507
0.0	0.751	0.751	0.751	0.751

Table 4: Numerical values for the datapoints in Figure 3 (left panel). Noisy CIFAR-10 dataset: Generated label accuracy of RCGAN, RCGAN-U, unbiased GAN and biased GAN.

Noise ($1 - \alpha$)	RCGAN	RCGAN-U	unbiased GAN	biased GAN
0.8	7.8	7.58	4.37	7.6
0.6	7.85	7.56	4	7.68
0.4	8.05	8.03	4	7.75
0.2	8.11	8.12	6	7.91
0.0	8.13	8.13	8.13	8.13

Table 5: Numerical values for the datapoints in Figure 3 (right panel). Noisy CIFAR-10 dataset: Inception score of RCGAN, RCGAN-U, unbiased GAN and biased GAN.

	label accuracy 0.2	label accuracy 0.3	label accuracy 0.4	label accuracy 0.5
RCGAN+y				
RCGAN				
RCGAN-U				
Unbiased				
Biased				

Figure 4: Images generated from the RCGAN+y, RCGAN , RCGAN-U, Unbiased and Biased GANs trained using noisy MNIST dataset, where class labels are flipped uniformly at random with probability $1 - \text{`real label accuracy'}$, under the uniform flipping model.

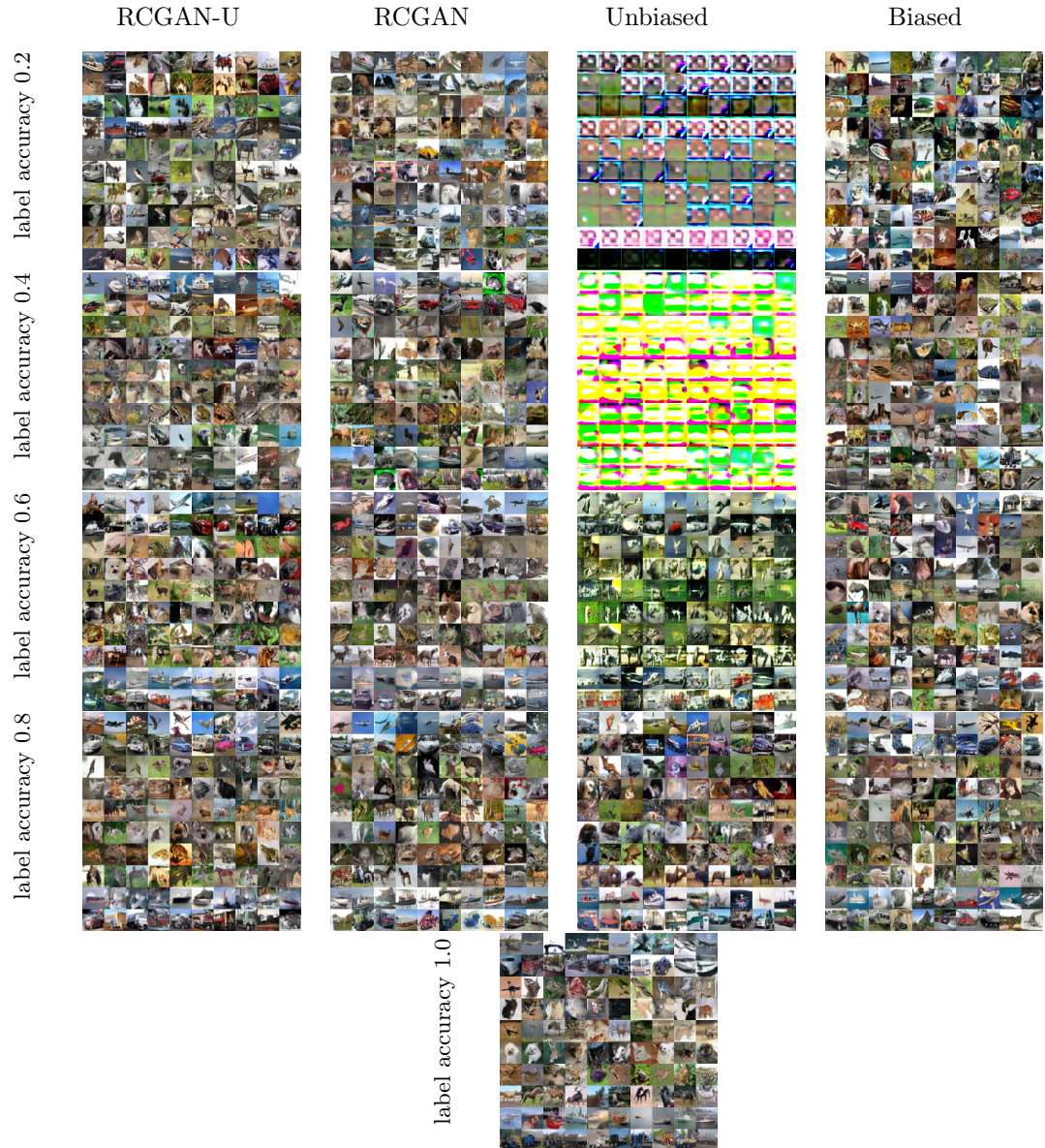


Figure 5: Images generated from the RCGAN-U, Unbiased and Biased GANs trained using noisy CIFAR-10 dataset, where class labels are flipped uniformly at random with probability $1 - \text{real label accuracy}$, under the uniform flipping model.